Functional analysis of cutinase transcription factors in *Fusarium verticillioides*

Minghui Peng[1,2,3], Jiajia Wang[1], Xiange Lu[1,4], Meiduo Wang[1], Gaolong Wen[1], Congxian Wu[5], Guodong Lu[2], Zonghua Wang[1,2,3*], Won Bo Shim[6*] and Wenying Yu[1,2*]

Abstract

Fusarium verticillioides is an important pathogen of maize and causes serious yield losses and food safety issues worldwide. *F. verticillioides* produces highly toxic mycotoxin Fumonisin B1 (FB1) in infested commodities which makes these food and feeds unsafe for humans and animals. For pathogenic fungi to successfully penetrate its plant hosts, the pathogen secretes hydrolytic enzymes that can facilitate penetration into the plant cutin layer. However, there is limited information on how cutinases transcriptionally regulated to impact *F. verticillioides* pathogenicity. In this study, our aim is to functionally characterize cutinase transcription factors that regulate key cutinase activities that are directly associated with *F. verticillioides* pathogenicity and FB1 biosynthesis. Gene deletion of cutinase transcription factor *FvCTF1α* did not affect the growth and morphology of the fungal mycelia on CMII medium, whereas the conidiation, utilization of sodium acetate and sodium oleate, stress tolerance against cell wall interfering agent and the cutinase and pectinase activities in the Δ*Fvctf1α* mutant were negatively impacted. FvCtf1α regulates the expression of induced cutinase genes *FvCUT1* and *FvCUT4* by binding to their GC-rich promoters. In addition, FvCtf1α, containing a novel function in regulating FB1, interacts with the promoter of *FvFUM1* and *FvFUM6* to down-regulate the expression of *FvFUM1* and *FvFUM6*, resulting in decreased production of FB1 in the Δ*Fvctf1α* strain. Δ*Fvctf1α* exhibited decreased pathogenicity in maize due to the down-regulation of pathogenicity-related genes as well as key downstream cutinase genes *FvCUT3* and *FvCUT4* in *F. verticillioides*. We also demonstrated that FvCtf1α regulated *FvCUT3* and *FvCUT4* differently; *FvCUT4* via direct regulation while *FvCUT3* via indirect regulation by interacting with FvFarB, a homologous protein of FvCtf1α. Moreover, RNA-seq analysis showed that FvCtf1α was associated with many pathways, such as fatty acid metabolism, carbon source utilization, cell wall integrity, oxidative stress, and fumonisin synthesis in *F. verticillioides*. Our study demonstrated that FvCtf1α was not only involved in the regulation of cutinases but also a broad spectrum of pathways that ultimately affect *F. verticillioides* virulence and mycotoxin biosynthesis.

Keywords *F. verticillioides*, FvCtf1α, Cutinase, Fumonisins, Pathogenicity

*Correspondence:
Zonghua Wang
wangzh@fafu.edu
Won Bo Shim
wbshim@tamu.edu
Wenying Yu
wenyingyu2004@126.com
Full list of author information is available at the end of the article

Peng *et al. Phytopathology Research*   (2024) 6:48

Page 2 of 18

Background

Cutin is the main structural component of the plant cuticle, a polymer consisting of hydroxy and epoxy fatty acids of n-C16 and n-C18 types (Kolattukudy 2001). Cutinases hydrolyze substrates such as p-nitrophenyl palmitate (pNPP), p-nitrophenyl butyrate (pNPB), and triglycerides (Martinez et al. 1992). The role of cutinases and their transcription factors in fungal pathogenicity against plants remains ambiguous. Some fungal pathogens secrete cutinases that hydrolyzes ester bonds from fatty acid polymers, thus facilitating fungal penetration through the cuticle (Hynes et al.2006). Four promoter elements involved in cutinase gene regulation are a positive-acting G-rich Sp1-like element, a silencer binding a basal transcription factor, and two overlapping palindromic sequences (palindrome 1 and palindrome 2) (Kämper et al. 1994; Li et al. 2002). Palindrome 1 (Pal 1) remains repressed until induced by cutin monomers (Li et al. 2002), while palindrome 2 (Pal 2) is the sequence that confers inducibility by plant cuticular monomers hydroxy fatty acids (Li and Kolattukudy 1997). Based on the binding preference to different *cis*-elements, especially the two overlapping palindromes in the cutinase gene promoter under varying environmental conditions, cutinase transcription factors (CTFs) are divided into four types, *i.e.*, palindrome-binding protein (PBP), Ctf1α, Ctf1β, and Ctf2, which regulate the expression of two cutinase types (constitutive expression and induction expression). PBP binds to Pal 1, while both Ctf1α and Ctf1β, which contain a Cys6Zn2 binuclear cluster motif, bind to Pal 2. Ctf2 binds to the *cis*-element located between the TATA box and the transcription initiation sites. In the absence of cutin monomers, PBP binds only to Pal 1 of the induction expression cutinase promoter to keep the gene repressed. However, in the presence of cutin monomers, Ctf1α phosphorylation displaces PBP (the repressor) from Pal 1 binding, thereby leading to the inactivation of dominant inhibitor PBP, and selectively binds to Pal 2, which induces gene expression (Li et al. 2002). Ctf1β usually can only bind to Pal 2 leading to the activation of constitutive expression cutinase genes and the production of low levels of cutin monomers. Ctf1β usually regulates constitutive expression cutinases, but if PBP does not preemptively bind to their sites, CTF1β can also regulate the induction of cutinase expression.

For example, if Pal 1 of the induction expression cutinase gene cannot bind to PBP, such as in the case of nucleotide substitutions in Pal 1, Ctf1β may bind to Pal 2 of the induction expression cutinase (Li et al. 2002). During the infection process in *Fusarium solani* f. sp. *pisi* virulent strains, the contact of a fungal spore with cutin, produced by small amounts of constitutively expressed cutinase, triggers the induction of cutinase transcription within minutes (Köller et al. 1982; Woloshuk and Kolattukudy 1986).

In addition to the induction of plant cuticular components, cutinase expression is under catabolite repression by glucose (Lin and Kolattukudy 1978). Glucose is involved in the regulation of cutinase expression by CTF. In a glucose-depleted condition, Ctf1α binds to its target sequence whether or not induced by cutin hydrolysate. Ctf2 binds to the *cis*-elements located between the TATA box and the transcription initiation sites in *F. solani*, which may be another gene-specific activating or repressing DNA-binding protein involved in cutinase gene regulation, potentially mediating glucose repression. *CUT1* of *F. solani* f. sp. *pisi* is also under glucose catabolite repression (Li et al. 2002). Altogether, Ctf1α can compete for PBP on cutin induction or Ctf2 can regulate the induction expression cutinase on the glucose-depleted situation.

Homologs of Ctf1 and Ctf2 have been found in several plant fungal pathogens, including *Aspergillus nidulans*, *Nectria haematococca*, *Fusarium oxysporum* f. sp. *lycopersici*, and *Magnaporthe oryzae* (Li et al. 2002; Hynes et al. 2006; Bravo-Ruiz et al. 2013; Bin Yusof et al.2014). FarA, the homolog of Ctf1α in *Aspergillus oryzae*, has conserved functions in the lipolytic system and fatty acids (Hynes et al. 2006; Garrido et al. 2012). These Ctf1 and Ctf2 orthologs are also present in human pathogenic yeast *Candida albicans* and alkane-assimilating yeast *Yarrowia lipolytica*, where they are involved in fatty acid utilization (Rocha et al. 2008; Ramírez et al.2009; Poopanitpan et al. 2010). Ctf1, a Ctf1α homolog, of the stem pathogen *F. solani* regulates *CUT1* and *LIP1* genes that are essential for virulence (Bravo-Ruiz et al. 2013), but Ctf1α of the root pathogen *F. oxysporum* is not essential for its virulence (Rocha et al. 2008). FarA and FarB of *A. nidulans*, two proteins with homology to Ctf1α, regulate the expression of genes implicated in the metabolism of short-chain and long-chain fatty acids, respectively (Hynes et al. 2006). FarA is implicated in the expression of cutinase protein Cut1 and hydrophobic surface-binding protein HsbA, required for the degradation of biodegradable plastic, butylene succinate-co-adipate (PBSA), as well as in the expression of lipolytic genes such as mono- and di-acylglycerol lipase *MDLB* and triacylglycerol lipase *TGLA* for lipid hydrolysis in *A. oryzae* (Garrido et al. 2012).

DNA motif identification plays a fundamental role in the elucidation of regulatory mechanisms of transcription factors. Among the many reported motifs, the AGGGG motif (G-box) has been observed in the promoters of fungal chitinase, cutinase, and many other genes (Kämper et al. 1994; Chen et al. 2021). The G-box motif in *N. haematococca* cutinase gene promoter is required

Peng *et al. Phytopathology Research*   (2024) 6:48

Page 3 of 18

for maintaining the basal level of cutinase gene transcription (Kämper et al. 1994). In addition, the C2H2-type zinc finger protein in *Y. lipolytica* Mhy1 and *Trichoderma atroviride* Seb1 also bind to the G-box motif in stress-response elements (Hurtado and Rachubinski 1999; Peterbauer et al. 2002). Despite this information, mechanistic insights into how the G-box binding transcription factor governs fungal infection remain unexplored. Gene induction by cutin monomers is regulated by Ctf1α, most likely a dimeric DNA-binding protein with a palindromic recognition site CCGAGG in *F. solani* (Li et al. 2002). FarA and FarB of *A. nidulans*, two proteins with homology to Ctf1α, bind in vitro to the same core DNA element that mediates the binding of the *F. solani* Ctf1α (Li and Kolattukudy 1997, Lin et al. 2022; Hynes et al. 2006).

The fungal pathogen *F. verticillioides* can cause significantly damaging grain diseases worldwide, particularly in China. The presence of *F. verticillioides* in grain can cause both substantial yield loss and grain contamination by Fumonisin B1 (FB1), a mycotoxin with significant pathological consequences for livestock and potentially for humans. The role of cutinase in *F. verticillioides* virulence and FB1 biosynthesis is not clearly defined. Although studies of Ctfs and Cuts had been performed in phytopathogenic fungi, such as *F. solani* (Li and Kolattukudy 1997, Lin et al. 2022), their complex regulatory mechanism in *F. verticillioides* on pathogenicity remains unclear. Our previous studies found that FvCtf1α regulates the production of toxin FB1. In this study, our aim was to characterize the role of *F. verticillioides* CTFs, mainly FvCtf1α, in expression of cutinases, as well as virulence and mycotoxin production.

Results

FvCTF1 and *FvCUT* genes of *F. verticillioides*

In the *F. verticillioides* genome, 12 cutinase genes (including *FvCUT1, FvCUT3, FvCUT4*), one cutinase palindrome-binding protein (*CPBP*), four Ctf1α (including *FvCTF1α* and *FvFARA*), and seven *FvCTF1β* (including *FvFARB*) were found. Except for one *CTF1β* and three cutinases, all other genes were detected by RNA-seq analysis in infected maize kernels and CMII medium (Table 1). *FvCPBP, FvFARA, FvCTF1α, FvCTF1αC, FvFARB, FvCTF1β,* and *FvCUT3* were constitutively expressed under different conditions according to RNA-sequencing data, and their expressions were significantly induced when *F. verticillioides* infected maize kernel (Table 1).

Identification of FvCtf1α as a transcription factor for cutinases *FvCUT1* and *FvCUT4* in *F. verticillioides*

When blasting Ctf1α and Ctf1β protein sequences of the pea stem pathogen *F. solani* to the *F. verticillioides*

genome database, we found only one homologous protein (FVEG_00228) with similarities of 29.62% and 27.51%, respectively. Functional domain analysis revealed that FVEG_00228 contained two conserved domains: GAL4-like Zn(II)2Cys6 and a fungal-specific transcription factor domain (Fungal trans) (Additional file 1: Figure S1a). Moreover, amino acids 341-373 of the FVEG_00228 protein sequence were predicted to be a bipartite nuclear localization signal (NLS). A phylogenetic tree was generated with FvCtf1α homologs from nine ascomycete fungi cutinase transcription factors. The results revealed that FvCtf1α was most similar to the proteins FoCtf1 and FsCtf1β (Additional file 1: Figure S1b). Therefore, FVEG_00228 was termed as FvCtf1α.

To examine the transcriptional activity of FvCtf1a, a yeast two-hybrid assay was performed. FvCtf1α exhibited self-activation activity in yeast transformants harboring the BD-FvCtf1α/pGADT7 vectors (Fig. 1a). To confirm the subcellular localization of FvCtf1α, the FvCtf1α-GFP vector was transformed into the ΔFvctf1α protoplast. FvCtf1α-GFP was observed to co-localize with the nucleus stained by DAPI (Fig. 1b), indicating that it localized in the nucleus of *F. verticillioides*. These results suggested that FvCtf1α is a transcription factor.

To characterize the functional roles of FvCtf1α in *F. verticillioides*, the *FvCTF1α* gene was deleted using a split-marker approach (Additional file 1: Figure S2a). The ΔFvctf1α mutants were first screened by PCR (Additional file 1: Figure S2b) and further confirmed by Southern blot assay (Additional file 1: Figure S2c). To verify that the phenotypic defects in the mutants were caused by the targeted gene deletion, a gene-complementation strain ΔFvctf1α-C was generated and further confirmed by qRT-PCR (Additional file 1: Figure S2f).

The corresponding homologs of four *A. nidulans* cutinase genes (*AnCUT1-AnCUT4*) were identified in *F. verticillioides*, termed as *FvCUT1–FvCUT4*. Functional domain analysis demonstrated that FvCut1–FvCut4 contained one cutinase domain and a signal peptide (Additional file 1: Figure S1c). However, *FvCUT2* was not expressed in either CMII or kernel medium, according to RNA-sequencing data. Compared with the wild-type strain Fv7600, the expression levels of *FvCUT1* and *FvCUT4* in ΔFvctf1α were down-regulated, while that of *FvCUT3* remained unaffected (Table 1). In addition, the expression levels of the four cutinase genes (*FvCUT1–FvCUT4*) were further assayed by qRT-PCR with or without cutin induction. The results showed that only three of these (excluding *FvCUT2*) were found to encode active cutinases (Fig. 1c–e). Therefore, a yeast one-hybrid assay was used to detect the relationships between the transcription factor FvCtf1α and three cutinase genes (*FvCUT1, FvCUT3,* and *FvCUT4*). The results showed

Table 1 The expression of cutinase transcription factor and cutinase gene in *Fusarium verticillioides* on different medium and the effect of Δ*Fvctf1α* mutant on kernel medium

Genes ID	Annotation	WT in CMII (2 d)	WT in kernel (10 d)	Δ*Fvctf1α* in kernel (10 d)	Log$_2$ (fold change) in kernel (Δ*Fvctf1α*/WT)	Log$_2$ (fold change) of WT (kernel/CMII medium)
FVEG_00478	*CPBP*	40.39	88.88	33.82	-1.39	1.14
FVEG_16071	*FvFARA*	51.57	1635.69	1623.10		4.99
FVEG_00228	*FvCTF1α*	7.78	316.31	0	Knock out	5.35
FVEG_05852	*FvCTF1αA*	1.09	84.35	66.50		6.27
FVEG_03397	*FvCTF1αB*	0.98	66.16	35.65	-0.89	6.08
FVEG_11995	*FvCTFf1αC*	10.64	321.01	233.72		4.92
FVEG_07971	*FvFARB*	69.39	3315.96	2137.42		5.58
FVEG_17758	*FvCTF1β*	4.81	137.39	149.39		4.84
FVEG_16361	*FvCTF1βA*	1.33	5.47	3.50		2.04
FVEG_09360	*FvCTF1βB*	0.43	24.75	10.74	-1.20	5.85
FVEG_12998	*FvCTF1βC*	0.52	55.56	22.43	-1.30	6.74
FVEG_12179	*FvCTF1βD*	0.00	0.00	0.00		
FVEG_03395	*FvCUT1*	0.00	2569.18	533.11	-2.26	up
FVEG_12346	*FvCUT2*	0.00	0	0		
FVEG_13638	*FvCUT3*	554.33	3048.44	4088.98		2.46
FVEG_09653	*FvCUT4*	1.07	1025.52	205.92	-2.32	9.19
FVEG_00397	*FvCUT5*	0.04	16.16	37.77	1.22	8.66
FVEG_03308	*FvCUT6*	0.00	65.00	173.16	1.41	up
FVEG_03351	*FvCUT7*	0.00	60.15	29.21	-1.04	up
FVEG_09293	*FvCUT8*	6.11	79.60	103.78		3.70
FVEG_10265	*FvCUT9*	6.63	160.82	139.30		4.60
FVEG_13534	*FvCUT10*	2.45	432.05	283.45		7.46
FVEG_00396	*FvCUT*	0.12	0	0		
FVEG_10728	*FvCUT*	0.00	0.35	0		

that FvCtf1α can bind to the promoters of *FvCUT1* and *FvCUT4* cutinase genes (Fig. 1f). Further analysis using the Multiple EM for Motif Elicitation (MEME) program revealed that FvCtf1α can bind to the GC-box (GCGC-CSC) region in the promoters of *FvCUT1* and *FvCUT4* cutinase genes (Fig. 1g). Thus, the results indicate that FvCtf1α is a transcription factor for cutinases *FvCUT1* and *FvCUT4*.

FvCtf1α regulates *F. verticillioides* cutinase genes under different conditions

To test whether FvCtf1α regulates the expression of the three cutinase genes (*FvCUT1*, *FvCUT3*, and *FvCUT4*) under cutin induction or H$_2$O$_2$ stress, we compared their expression patterns in the Δ*Fvctf1α* mutant and wild-type (WT) strains using qRT-PCR. Firstly, the expression profiles of these cutinase genes were measured at different stages of cutin induction. Although *FvCUT1*, *FvCUT3*, and *FvCUT4* in the Δ*Fvctf1α* mutant were slightly up-regulated compared to the WT without cutin induction at early stages, after 1 h cutin induction,

the expressions of *FvCUT3* and *FvCUT4* were significantly increased (2 to 8-fold) in the wild-type. However, the expressions of *FvCUT1*, *FvCUT3*, and *FvCUT4* in Δ*Fvctf1α* did not change. The induced expression peaks of *FvCUT1*, *FvCUT3*, and *FvCUT4* were reached at 3–5 h of cutin induction and decreased at 12 h in WT, while the expression levels for Δ*Fvctf1α* remained unchanged (Fig. 1c-e) during these stages. However, after 3 days of cutin induction with low H$_2$O$_2$ stress, *FvCUT1* and *FvCUT4* were abundantly induced in WT, especially for the expression of *FvCUT1*, but the expression levels in the Δ*Fvctf1α* mutant were reduced (Fig. 1h). Therefore, we hypothesize that FvCtf1α positively regulates *FvCUT* (*FvCUT1*, *FvCUT3*, and *FvCUT4*) gene expression under cutin induction, and more specifically regulates *FvCUT1* and *FvCUT4* under cutin induction with low oxidative stress. Simultaneously, under cutin induction with low H$_2$O$_2$ stress, the expression levels of three genes, including β-oxidation (*FvPOT1*) and peroxisome biogenesis (*FvPEX5* and *FvECL1*), were reduced in the Δ*Fvctf1α* mutants (Fig. 1i). These observations suggest

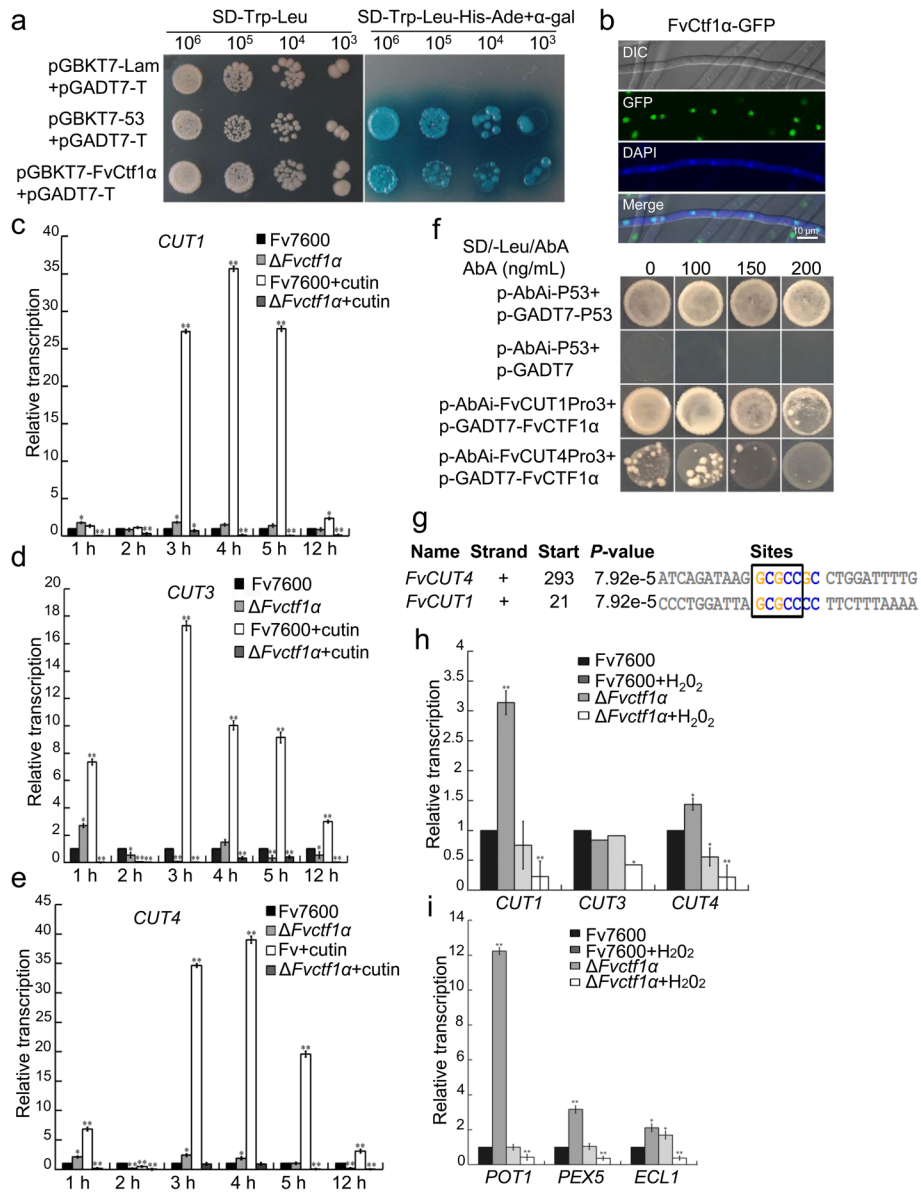Peng *et al. Phytopathology Research*   (2024) 6:48

Page 5 of 18

Fig. 1 Identification of transcription factors FvCtf1α in the regulation of *FvCUT1* and *FvCUT4* in *F. verticillioides*. **a** Self activation activity was verificated by yeast two-hybrid assays. Yeast transformants harboring the BD-FvCtf1α/pGADT7 vectors were assayed for growth on selective plates (SD/-Leu/Trp/His/Ade), and X-α-Gal added to test for β-galactosidase (LacZ) activities. X-α-Gal: 5-Bromo-4-chloro-3-indolyl-α-D-galactos ide. The pGBKT7-53/pGADT7-T and pGBKT7-Lam/pGADT7-T were used as positive and negative controls, respectively. Scale bars: 10 μm. **b** The localizations of CTF transcription factor FvCtf1α was observed in the nucleus with the nucleus stained by DAPI. **c–e** The expression patterns of three cutinase genes within 12 h of cutin induction: the expression levels of cutinase genes *FvCUT1*, *FvCUT3*, and *FvCUT4* in WT and mutants were detected at 1, 2, 3, 4, 5, and 12 h, respectively. **f** FvCtf1α can bind the promoters of the two cutinase genes *FvCUT1* and *FvCUT4* by yeast one-hybrid. pAbAi::*FvCUT1*pro vector, pAbAi::*FvCUT4*pro vector, and pGADT7-FvCtf1α were constructed and the Y1H-Gold strain was sequentially transferred into two vectors, first transferred into the pAbAi::*FvCUT1*pro vector (or pAbAi::*FvCUT4*pro vector), selecting with SD/-Ura medium, and re-introduced into the pGADT7-FvCtf1α vector, selecting with SD/-Ura media with 0, 100, 150, 200 ng/mL Aureobasidin A (AbA).The vector pair pAbAi::p53pro/ p53-pGADT7 transformants serves as the positive control and the vector pAbAi::p53pro/pGADT7 transformants serves as the negative control. **g** FvCtf1α can bind the promoters of the two cutinase genes *FvCUT1* and *FvCUT4* at GC-rich site by Multiple EM for Motif Elicitation (MEME) software. $p < 0.01$. **h** The expression of *FvCUT1*, *FvCUT3*, *FvCUT4* were assayed by qRT-PCR under low H_2O_2 stress. **i** The expression level of three genes including β-oxidation (*FvPOT1*) and peroxisome biogenesis (*FvPEX5*, *FvECL1*) were compared by WT and Δ*Fvctf1α*, respectively. The transcription level of the target gene was determined using qRT-PCR assay and calculated using the $2^{-\Delta\Delta Ct}$ method with *TUB2* as reference gene. Analysis of variance is three independent repeated experiments and asterisks represent a significant difference. (*t*-test, *: $p < 0.05$, **: $p < 0.01$)

Peng *et al. Phytopathology Research*   (2024) 6:48

Page 6 of 18

that the Δ*Fvctf1α* mutant may not respond to low H_2O_2 stress as it does not stimulate the ROS clearance function of peroxisomes.

Investigating the relationship between FvCtf1α and other FvCtfs

To further investigate the regulatory mechanism of constitutively expressed and induced cutinase genes by different cutinase transcription factors (FvCtfs) in *F. verticillioides*, other FvCtfs were studied. The homologous proteins FvCtfs FarA and FarB of *A. nidulans* were found through a blast search in the *F. verticillioides* genome, with gene numbers FVEG_16071 (*FvFARA*) and FVEG_07971 (*FvFARB*). Like FvCtf1α, both FvFarA and FvFarB contain two domains: the GAL4 domain and the transcription factor domain (Fungal trans) (Additional file 1: Figure S1a). DAPI staining was used for nuclear localization markers. The green fluorescence of FvFarA-GFP and FvFarB-GFP colocalized with the nuclear blue light signal, respectively, indicating that FvFarA-GFP and FvFarB-GFP of *F. verticillioides* were also localized in the nucleus (Fig. 2a). Fluorescence could be observed in the hyphae of the transformants containing FvCtf1α-NYFP and FvFarB-CYFP, but not in the hyphae of the transformants containing FvCtf1α-NYFP and FvFarA-CYFP. This indicates that FvCtf1α can interact with FvFarB but not with FvFarA in *F. verticillioides* (Fig. 2b).

FvCtf1α affects fatty acid metabolism and carbon source utilization

To test whether *F. verticillioides* FvCtf1α affects the utilization of various carbon nutrients, we cultured WT, Δ*Fvctf1α* mutants, and Δ*Fvctf1α-C* on minimal medium (MM) agar plates with different carbon sources. The results showed that there was no significant difference in the growth rates of the Δ*Fvctf1α* mutants compared with that of the WT and the complementary strain Δ*Fvctf1α-C* when ethanol absolute,

glycerol, and sodium butyrate were used as the sole carbon sources (Fig. 3a). However, the vegetative growth rates of Δ*Fvctf1α* were significantly reduced on sodium acetate and sodium oleate medium when compared with those of the WT and Δ*Fvctf1α-C* strains (Fig. 3a–d). Growth inhibition on sodium acetate and sodium oleate medium were more drastic for Δ*Fvctf1α* than other carbon sources (Fig. 3c, d). These results suggest that Δ*Fvctf1α* mutants have defects in fatty acid metabolism and the utilization of certain carbon sources, such as sodium acetate and sodium oleate.

Three carbon metabolism pathway-related genes, *FvFBP1* (FVEG_03829), *FvICL1* (FVEG_02611), and *FvFOX2* (FVEG_04199), were selected for further analysis. The results showed that their expression was significantly reduced in Δ*Fvctf1α* mutants (Fig. 3e). These observations suggest that the Δ*Fvctf1α* mutant may affect carbon metabolism due to significantly reduced expression levels of carbon metabolism-related genes.

Deletion of *FvCtf1α* resulted in a conidial production defect

To investigate whether the sporulation of Δ*Fvctf1α* mutants is affected, WT, Δ*Fvctf1α*, and Δ*Fvctf1α-C* were inoculated in potato dextrose agar (PDA) medium. The results showed that the sporulation of the Δ*Fvctf1α* mutants decreased significantly compared to the WT and the complementary strain Δ*Fvctf1α-C* (Fig. 3f). In addition, the expression of the conidia-related gene *FvCON7* (FVEG_10320) was significantly reduced in Δ*Fvctf1α* mutants (Fig. 4c). These results suggest that the effect of FvCtf1α on conidial production defects may be due to a significant decrease in the expression level of *FvCON7*.

FvCtf1α affects cell wall-degrading enzyme (CWDE) activity and contributes to cell wall integrity stress and H_2O_2 stress

The activity of three CWDE, including cutinase, pectinase, and cellulase, was assessed in Δ*Fvctf1α*. Compared
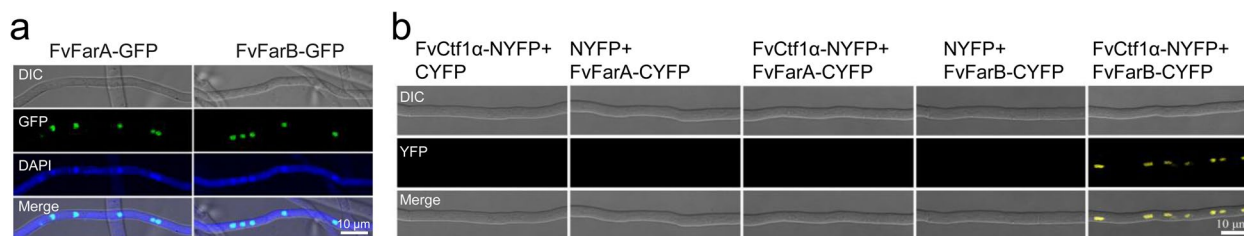

Fig. 2 Identification the relationship of FvCtf1α with other transcription factors CTFs. **a** The localizations of CTF transcription factor FvFarA-GFP and FvFarB-GFP were observed in the nucleus with the nucleus stained by DAPI, respectively. **b** The interaction of FvCtf1 with FvFarA or FvFarB analyses by BiFC fluorescence. Five plasmid pairs were co-transformed into wild-type Fv7600 protoplast, with three plasmid pairs FvCtf1α-NYFP and CYFP, NYFP and FvFarA-CYFP, NYFP and FvFarB-CYFP using as negative controls, while the plasmid pairs FvCtf1α-NYFP and FvFarA-CYFP, FvCtf1α- NYFP, and FvFarB-CYFP were used as tests. BiFC fluorescence images were captured on confocal laser scanning microscope. Scale bars: 10 μm
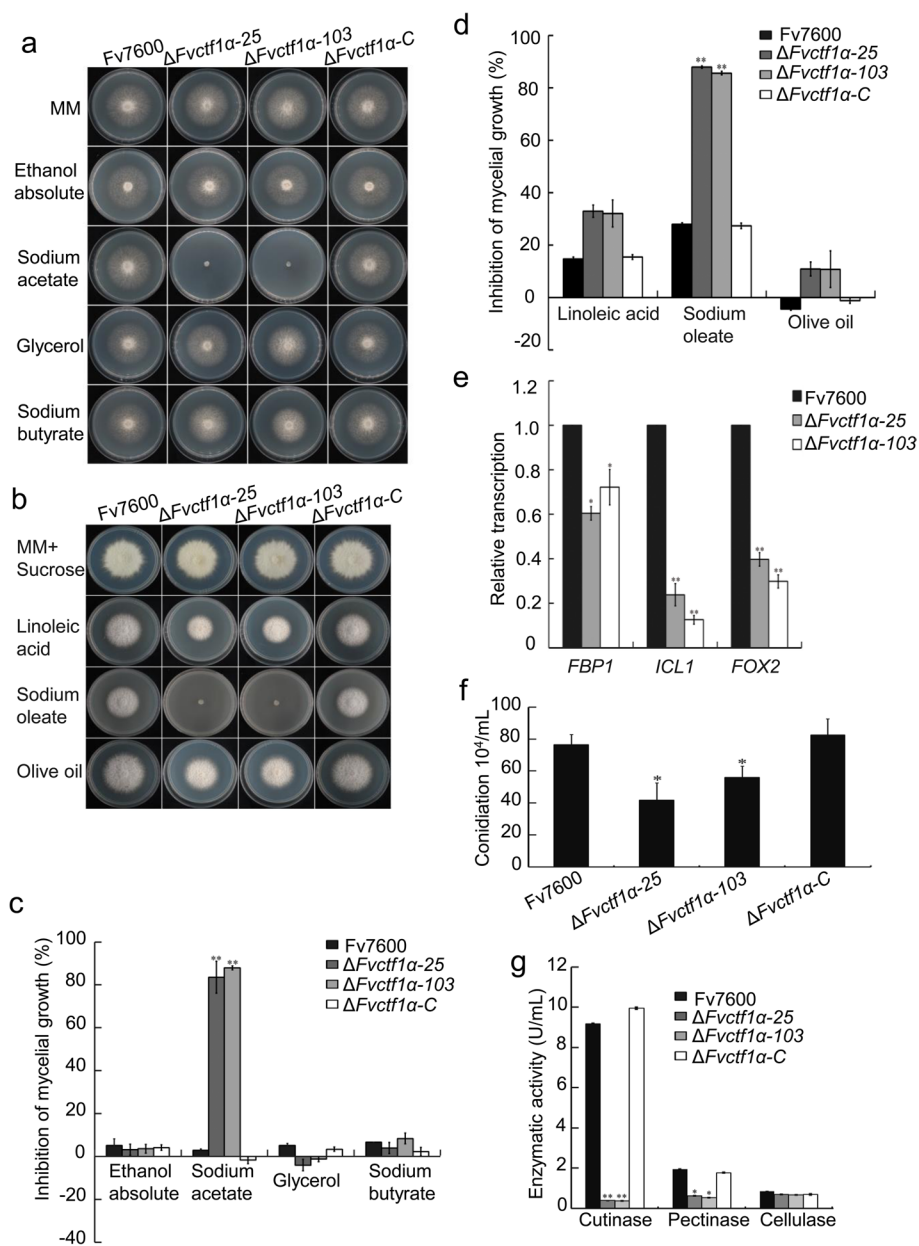
Fig. 3 Defect on carbon metabolic, producing conidia and cell wall degrading enzyme activity of Δ*Fvctf1α* deleted mutants. **a** To compare the nutrient utilization capacity of the WT and mutant strains, the vegetative growths of the strains were monitored on MM with short chain carbon, respectively. **b** The vegetative growths of the strains were monitored on MM with long chain carbon, respectively. **c**, **d** The colony diameters of the cultures were measured and inhibition of mycelial growth analyzed by *t*-test on short chain carbon, on long chain carbon. **e** The expression levels of the carbon metabolic related genes were significantly down-regulated in Δ*Fvctf1α* by qRT-PCR with the reference gene *TUB2* using the $2^{-\Delta\Delta Ct}$ method. **f** Measurement and statistical comparison of conidia from WT and mutant strains after inoculation on CMII at 28℃ for 3 days. Error bars denote standard deviations from three repeated experiments and asterisks represent a significant difference. **g** The activity of three cell wall degrading enzyme including cutinase, pectinase, and celluase were assessed in Δ*Fvctf1α* and WT, respectively. The experiment was performed three times with similar results and error bars represent the standard deviation and asterisks represent a significant difference (*t*-test, *: $p < 0.05$, **: $p < 0.01$)

with the WT, cutinase, and pectinase activities were significantly reduced in Δ*Fvctf1α*, but cellulase activity was not affected in Δ*Fvctf1α* (Fig. 3g).

To explore the roles of FvCtf1α in the regulation of different stress responses, mutant strains were cultured in MM containing SDS, CFW, CR, or H_2O_2. The results

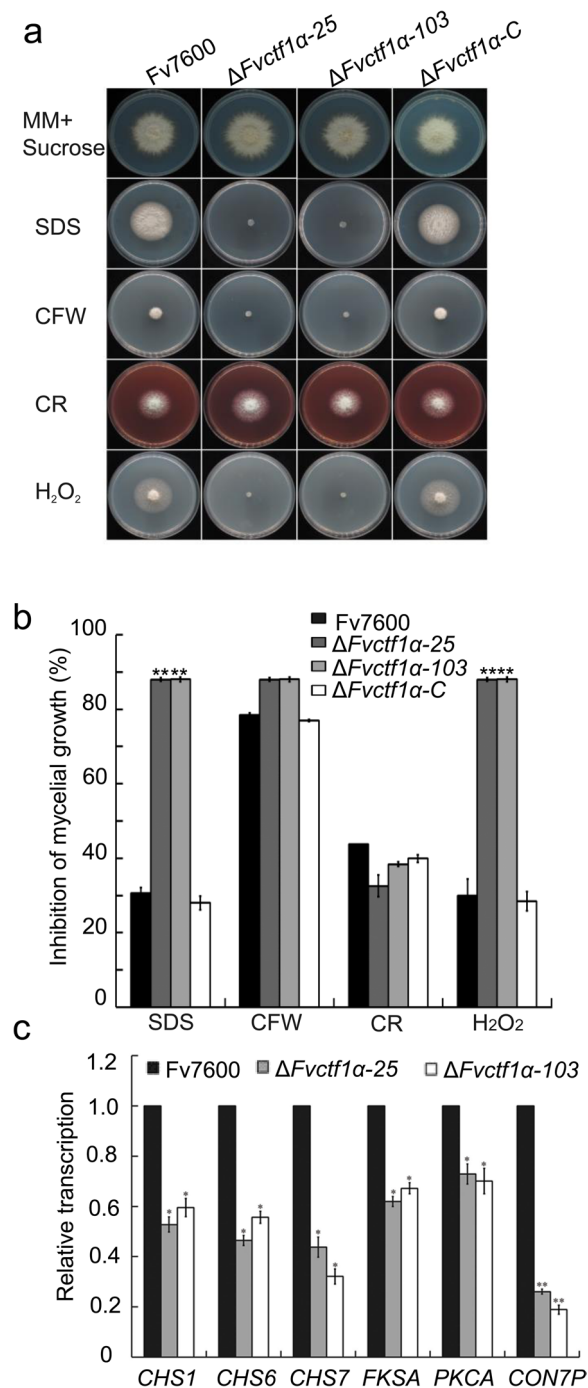Peng *et al. Phytopathology Research*   (2024) 6:48

Page 8 of 18

Fig. 4 FvCtf1α alters tolerance to cell wall and oxidative stress. **a** The growth of colony were monitored for tolerance to cell wall and oxidative stress on MM by addition with CR, CFW, SDS, or H_2O_2. CR: congo red, CFW: calcofluor white, SDS: sodium dodecyl sulfate. **b** The inhibition rates of mycelial growth under cell wall and oxidative stresses were analyzed and subjected to statistical analysis, respectively. **c** The expression level of six cell wall synthase related genes *FvCHS1, FvCHS6, FvCHS7, FvFKA, FvPKCA,* and one conidia related gene *FvCON7* were compared by Δ*Fvctf1α* and WT, respectively. qRT-PCR was used to quantify transcript level of genes to the reference gene *TUB2* using the $2^{-\Delta\Delta Ct}$ method. Error bars represent the standard deviation and asterisks represent a significant difference (*t*-test, *: $p < 0.05$, **: $p < 0.01$)

Six cell wall synthase-related genes, chitin synthases (*CHS*), *FvCHS1* (FVEG_02839), *FvCHS6* (FVEG_07280), *FvCHS7* (FVEG_07296), *FvFKA* (FVEG_12144), *FvP-KCA* (FVEG_06268), and *FvCON7* (FVEG_10320) were selected for further analysis. Compared to the WT, the expression levels of these six cell wall synthase-related genes were significantly reduced in Δ*Fvctf1α* mutants (Fig. 4c). The results suggest that the effect of Fvctf1α on cell wall integrity may be due to a significant decrease in the expression level of cell wall synthase genes.

FvCtf1α is a regulatory transcription factor for fumonisin synthesis genes and is important for normal FB1 biosynthesis

The effect of *FvCTF1α* gene deletion on fumonisin B1 (FB1) biosynthesis was investigated. The wild-type and Δ*Fvctf1α* mutant strains were inoculated in solid maize powder medium, and the concentration of FB1 produced in mycelium and medium was detected after culturing at 28℃ for 10 days, respectively. The results showed that the vast majority of FB1 was secreted extracellularly and accumulated in the medium (Fig. 5a). The FB1 secreted into the medium by the Δ*Fvctf1α* mutant was significantly lower than that of the wild-type, and FB1 accumulated in the mycelium showed the same trend (Fig. 5a). We further examined the expression levels of four key *FUM* genes including *FvFUM1, FvFUM8, FvFUM19* and *FvFUM21-* in the wild-type and Δ*Fvctf1α* mutant strains. The results showed that the expression levels of these four genes in the Δ*Fvctf1α* mutant were significantly lower than those of the wild-type strain (Fig. 5b).

To determine whether FvCtf1α is a regulatory transcription factor for FB1 synthesis genes, we conducted yeast one-hybrid (Y1H) assays to determine the interaction between FvCtf1α and each *FUM* gene. The results showed that FvCtf1α can bind to the promoters of 5 *FUM* genes: *FvFUM1, FvFUM2, FvFUM6, FvFUM14,* and *FvFUM16* (Fig. 5c). Further analysis by Multiple EM for Motif Elicitation (MEME) software revealed that FvCtf1α

showed that Δ*Fvctf1α* mutants were more sensitive to the chemical treatments of SDS and H_2O_2, and the inhibition rate under these two stresses increased significantly compared with the WT and Δ*Fvctf1α-C* strain (Fig. 4a, b). These findings indicate that FvCtf1α is involved in the response to cell wall integrity stresses and oxidative stress.
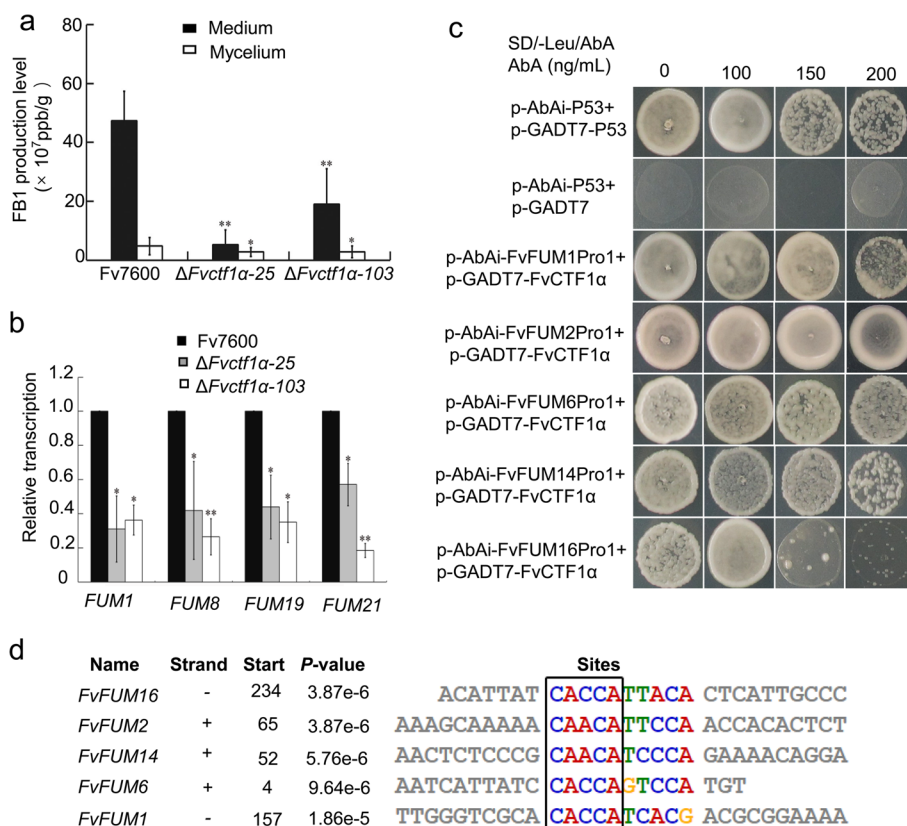
Fig. 5 FvCtf1α plays key role in fumonisin B1 (FB1) production. **a** FB1 levels in the samples were measured using the formula FB1/*TUB2* DNA. Surface sterilized B73 corn kernels were inoculated with the WT and mutant conidia suspensions and incubated for 10 d. FB1 levels were quantified using ELISA Kit. *F. verticillioides* biomass was quantified by measuring *F. verticillioides TUB2* DNA in samples. ELISA: enzyme-linked immunosorbent assay. **b** Relative *FUM* genes expression were compared by Δ*Fvctf1α* and WT, respectively. qRT-PCR was used to quantify transcript level of *FUM* genes to the reference gene *TUB2* using the $2^{-\Delta\Delta Ct}$ method. The experiment was performed three times. Error bars represent the standard deviation. (*t*-test, *: $p < 0.05$, **: $p < 0.01$). **c** FvCtf1α can bind the promoters of the five *FUM* genes *FvFUM1, FvFUM2, FvFUM6, FvFUM14,* and *FvFUM16* by yeast one-hybrid, respectively. pAbAi::*FvFUM1*pro, pAbAi::*FvFUM2*pro, pAbAi::*FvFUM6*pro, pAbAi::*FvFUM14*pro, pAbAi::*FvFUM16*pro vectors, and pGADT7-FvCtf1α were constructed. The Y1H-Gold strain was sequentially transferred into two vectors, first transferred into the pAbAi::*FvFUM1*pro vector (or pAbAi::*FvFUM2*pro vector), selecting with SD/-Ura medium, and reintroduced into the pGADT7-FvCtf1α vector, selecting with SD/-Ura media with 0, 100, 150, 200 ng/mL Aureobasidin A (AbA). The p53-AbAi vector transformants were used as the negative control and pAbAi::pro vector transformants as the positive control. **d** FvCtf1α can bind the promoters of the five *FUM* genes at CAMCA site by Multiple EM for Motif Elicitation (MEME) software

may bind to the CAMCA DNA element regions of the 5 *FUM* genes promoters (Fig. 5d). Y1H assays (Fig. 5c) and RNA-sequencing (Table 2) results confirmed that FvCtf1α was a new regulatory transcription factor of the FB1 biosynthesis genes.

FvCtf1α, FvCut4, and FvCut3 contribute to pathogenicity

To explore the role of FvCtf1α in the infection process of *F. verticillioides* on different crops, we first inoculated the mycelium blocks of the WT and Δ*Fvctf1α* strains on the stems of susceptible maize (B73) seedlings. The Δ*Fvctf1α* showed a severe decrease in pathogenicity after 7 days post-inoculation (dpi) when compared to the WT (Fig. 6a). Next, we inoculated WT and

Δ*Fvctf1α* mutant strains on maize leaves and used real-time quantitative PCR (qRT-PCR) to detect the expression of six resistance genes (*PRm3*, *PRm6*, *PR-1*, *PR-5*, *NPR1*, and *LOX10*) in the leaves 2 dpi. The expression levels of maize resistance genes were significantly up-regulated following Δ*Fvctf1α* mutant infection (Fig. 6b). Additionally, the susceptible sugarcane (badila) stem was inoculated with a toothpick soaked in a spore suspension of WT and Δ*Fvctf1α*. After 7 dpi at 28℃, we used ImageJ software to statistically analyze the disease area. The results showed that the pathogenicity of Δ*Fvctf1α* mutant was significantly reduced compared to the WT and complemented strain Δ*Fvctf1α*-C (Fig. 6c, d). These results indicate that the FvCtf1α is essential

Peng *et al. Phytopathology Research*   (2024) 6:48

Page 10 of 18

Table 2 DEG of *FUM* genes between Δ*Fvctf1α* mutants and WT

Genes ID	Annotation	Fold change in kernel (Δ*Fvctf1*/WT)	*p*-value
FVEG_00320	*FUM3*	-9.375643123	4.969e-05
FVEG_00325	*FUM14*	-8.544388533	1.446e-05
FVEG_00323	*FUM2*	-8.075059552	3.523e-05
FVEG_00321	*FUM10*	-7.896863031	7.433e-05
FVEG_00317	*FUM6*	-7.6246404	2.766e-05
FVEG_00316	*FUM1*	-7.39696999	6.868e-06
FVEG_00326	*FUM16*	-6.193645764	2.508e-06
FVEG_00327	*FUM17*	-6.032588819	8.151e-05
FVEG_00324	*FUM13*	-5.782155725	7.466e-05
FVEG_00329	*FUM19*	-5.492912372	1.938e-06
FVEG_00322	*FUM11*	-5.307275718	8.05e-05
FVEG_00328	*FUM18*	-4.91864426	1.245e-06

for the pathogenicity of *F. verticillioides* on the stem of maize and sugarcane.

Most fungal pathogens produce cutinases that can hydrolyze host cutin and promote pathogen invasion, especially to leaves. Thus, we further attempted to explore whether the loss of pathogenicity of the Δ*Fvctf1α* mutant was correlated to the function of cutinase genes. We tried to knockout three cutinase genes, *FvCUT1*, *FvCUT3*, and *FvCUT4*, to investigate the role of cutinase in pathogenicity. However, we only obtained Δ*Fvcut3* and Δ*Fvcut4* mutants, while *FvCUT1* knockout mutants were not obtained. No open reading frame (ORF) was detected in the Δ*Fvcut*3 and Δ*Fvcut*4 mutants by PCR assay, but the correct linkage UA was detected as an alternative insertion sequence (Additional file 1: Figure S3a, b). Subsequently, qRT-PCR assay confirmed that the genes knocked out in their respective mutants were not expressed (Additional file 1: Figure S3c, d). The deletion of *FvCUT3* and *FvCUT4* did not affect mycelial growth
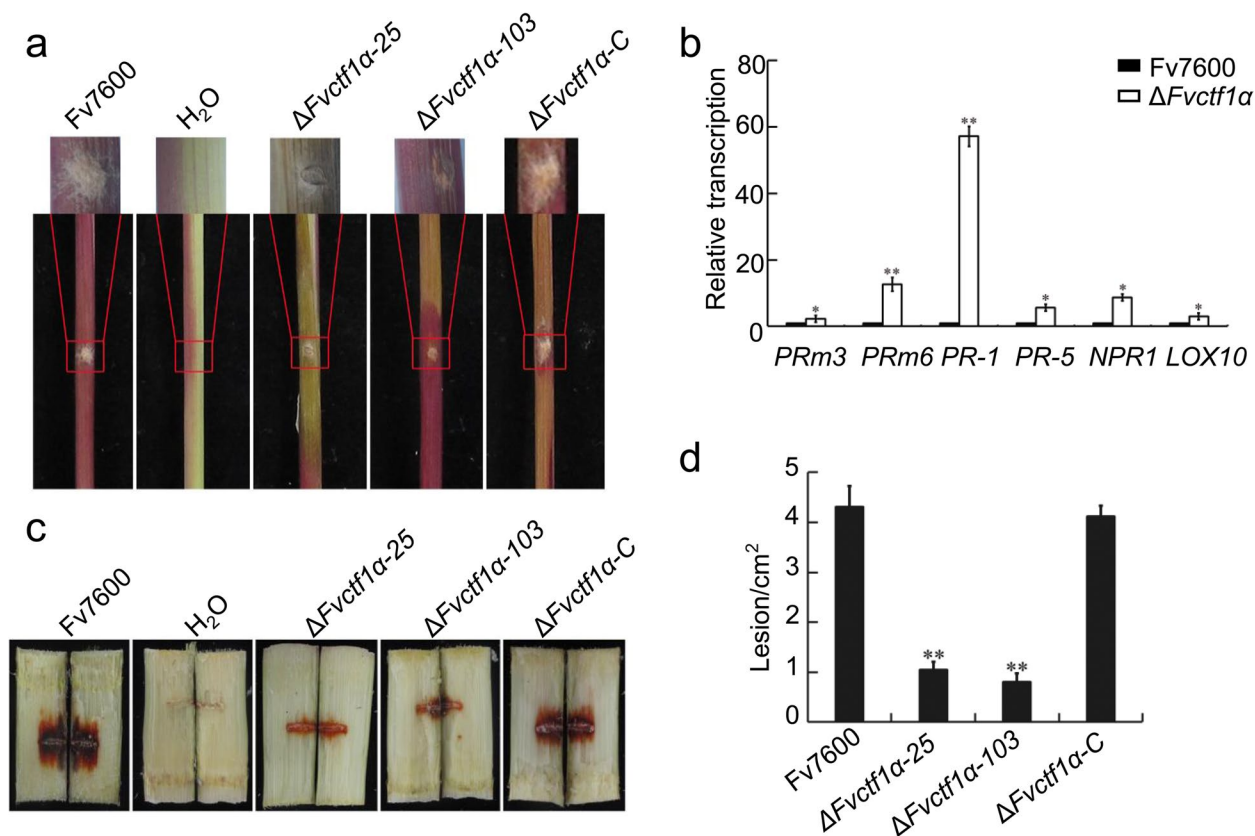

Fig. 6 FvCtf1α plays key role in pathogenicity. **a** The B73 maize seedling were inoculated with colony disk and then observed after 7 dpi. **b** The expression of relative six resistance genes of B73 maize by qRT-PCR were compared between Δ*Fvctf1a* and WT, respectively. qRT-PCR was used to quantify transcript level of genes to the reference gene *GAPDH* (X07156) using the $2^{-\Delta\Delta Ct}$ method. **c** Sugarcane was split longitudinally to visually inspect rot symptoms after 7 dpi. Sugarcane (badila) was inoculated with immersed conidia toothtip at the internodal region after 7 dpi. The cane were inoculated with sterile toothtip as a negative control. **d** The area of discoloration of split longitudinal section of cane was quantified by ImageJ software and subjected to statistical analysis. The experiment was performed three times. Error bars represent the standard deviation and asterisks represent a significant difference. (*t*-test, *: $p < 0.05$, **: $p < 0.01$)

in each case (Additional file 1: Figure S4a). However, the deletion of *FvCUT4* and *FvCUT3* did not affect pathogenicity on the stem of sugarcane but on maize leaves (Fig. 7, Additional file 1: Figure S4b, c). On the other hand, to investigate whether the deletion of two other *CTFs*, *FvFARA* and *FvFARB*, had an impact on pathogenicity, we constructed knockout mutants of these two genes (Additional file 1: Figure S2d–h). However, there was no difference in growth and pathogenicity between the wild-type and the two mutant strains (Additional file 1: Figure S5a–c).

FvCtf1α is involved in multiple metabolic pathways

To investigate genes whose expression levels are regulated by FvCtf1α, we conducted RNA-sequencing analysis on the ΔFvctf1α mutants at the maize-infested stage. Differential gene expression (DEG) analysis was conducted using cuffdiff v2.1.1 with parameters: -FDR (False Discovery Rate)=0.05 -library-norm-method classic-fpkm -u/-multi-read-correct-b/-frag-bias-correct. A gene that was considered to be differentially expressed must have at least 1.2-fold|Log$_2$fold change|variation between WT and ΔFvctf1α mutant. Our results found that 617 genes were down-regulated and 807 genes were up-regulated in the ΔFvctf1α mutant compared with the WT among the DEGs (Additional file 1: Figure S6a).

GO enrichment and KEGG enrichment pathways were further analyzed in DEGs. Using GO annotation and enrichment (Ye et al. 2018), the down- and up-regulated DEGs were enriched to 17 and 19 GO terms (Additional file 1: Figure S6b, c), respectively. The top 6 down-regulated enrichment pathways were mainly associated with carbohydrate metabolic processes, transmembrane transporter activity, transcription, catalytic activity hydrolase, and heme binding (Additional file 1: Figure S6b), while the top 5 up-regulated enrichment pathways were mainly classified into membrane, carbohydrate metabolic processes, transmembrane transporter activity, proteolysis, and hydrolase (Additional file 1: Figure S6c). Moreover, using KEGG annotation and enrichment (Dennis et al. 2003), the down- and up-regulated DEGs were enriched to 20 and 5 pathways (Additional file 1: Figure S6d, e), respectively. The top 5 down-regulated enrichment pathways were associated with biosynthesis of secondary metabolites, biosynthesis of antibiotics, microbial metabolism in diverse environments, carbon metabolism, fatty acid degradation, and arginine and proline metabolism (Additional file 1: Figure S6d). For the secondary metabolite FB1, all genes related to its metabolism are down-regulated (Table 2). However, their FDR were high in 5 up-regulated pathways (Additional file 1: Figure S6e). The analysis of enrichment pathways, combining both GO and KEGG enrichment, showed that the deletion of *FvCTF1α* affects transcription, membrane, carbon metabolism, and biosynthesis of secondary metabolites.

Discussion

Cutinases are extracellular enzymes that catalyze the hydrolysis of the ester bonds of cutin, suberin, lipids, and waxes. A variable number of genes encoding cutinase enzymes have been found, ranging from three to seventeen within a single organism (Skamnioti et al. 2008). In our study, RNA-seq analysis of *F. verticillioides* in CM medium and maize kernel identified one cutinase palindrome-binding protein (*CPBP*), four *CTF1α* (including

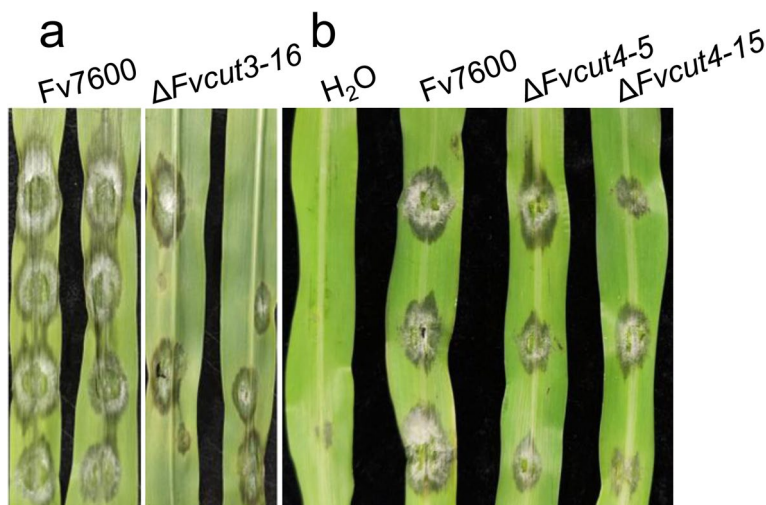
Fig. 7 FvCut3 and FvCut4 play a role in pathogenicity. **a**, **b** The B73 maize leaves were inoculated with colony disk and the infection leaf with water-logging of wide-type, ΔFvcut3,and ΔFvcut4 were observed after 5 dpi

FvCTF1α and *FARA*), six *CTF1β* (including *FARB*), and nine cutinase genes (Table 1). The divergent evolution of cutinase-encoding genes could lead to more efficient enzymes and better adaptation to different niches or conditions. In the CMII medium, transcription factors *CPBP*, *FvFARA*, and *FvFARB*, as well as *CUT* genes *FvCUT3*, were highly expressed in *F. verticillioides*. In addition, maize kernel infected by *F. verticillioides* induced the expression of many other *CTFs* and *CUT* genes, such as the transcription factor *FvCTF1α*, *FvCTF1αA*, *FvCTF1αB*, *FvCTF1αC*, *FvCTF1β*, *FvCTF1βC*, as well as *CUT* genes *FvCUT1*, *FvCUT4*, *FvCUT6*, *FvCUT7*, *FvCUT8*, *FvCUT9*, and *FvCUT10*. Our results also showed that FvCtf1α affected the fatty acid metabolism and the utilization of certain carbon sources, such as sodium acetate and sodium oleate. The specific mechanism of different cutinase expression in *F. verticillioides* still needs further research, whether it is consistent with *F. solani*, where makes a substrate-induced, catabolite-repressed cutinase (Lin and Kolattukudy 1978).

However, the role of cutinase in different pathogen species varies. Pea stem pathogen *F. solani* cutinase can help to breach the cuticular barrier of the host plant, playing a significant role in pathogenesis (Woloshuk and Kolattukudy 1986). Three *F. solani* cutinase genes, *FsCUT1*, *FsCUT2*, and *FsCUT3* share a high degree of identity. While *FsCUT2* and *FsCUT3* are expressed constitutively at basal levels (Lin et al. 2022), the expression of *FsCUT1* is strongly induced by cutin monomers and mediated by the zinc finger transcription factor Ctf1α in *F. solani* (Li and Kolattukudy 1997, Lin et al. 2022). Deletion of the *FsCUT1* resulted in decreased virulence in peas (Kämper et al. 1994; Li et al. 2002), and insertion of *FsCUT1* into *Mycosphaerella*, a pathogen that normally requires wounds on the papaya fruits surface to cause infection, allowed the transgenic strains to penetrate an intact surface (Dickman et al. 1989). *Magnaporthe grisea CUT2* was shown to be associated with pathogenicity (Skamnioti and Gurr 2007). Yeast *Pseudozyma antarctica* on the leaf may be utilizing an cutinase-like enzymes (CLEs) to extract fatty acids as nutrients, and leaf surfaces were heavily damaged by high concentrations of CLEs (Ueda et al. 2015). These CLEs can degrade tomato leaf cutin, enabling plant pathogens to easily invade leaves (Ueda et al. 2018, Ueda et al. 2021). However, numerous gene mutation studies have failed to show an essential role for cutinase in different pathogen species, such as *M. grisea CUT1* and *Botrytis cinerea* cutinase A (Sweigard et al. 1992; Van kan et al 1997). Unlike *F. solani* and *M. grisea* where only specific cutinase enzymes were linked to host infection, both *FvCUT4*, the inducible enzyme, and *FvCUT3*, the constitutive enzyme, were associated with *F. verticillioides* infection of maize leaves. Therefore,

compared with *F. solani* and *M. grisea*, *F. verticillioides* contains more cutinase genes and more complex mechanisms for regulating pathogenicity.

The presence of different binding sites for different transcription factors (TFs) in *CUT* genes, *e.g.*, CCTGCC/GGCAGG for *FARA* and *FARB*, GGAATTGGGGCATTGG for *NAPA*/*NF-Y1*, and GGC(n3)GCC for *CTF1*, result in their expression under different conditions (Kämper et al. 1994; Lin et al. 2022; Bermúdez-García et al. 2019). Some transcription factors recognize a DNA sequence with two inverted repeats of CGG elements, separated by a characteristic number of bases. It is recorded that some TFs recognize 5'-CGG(n)CCG with a spacer of different nucleotides, *e.g.*, the spacers for *GAL4*, *PUT3*, *PPR1*, and *LEU3* are 11, 10, 6, and 4 nucleotides, respectively (Zhang and Guarente 1994). Ctf1α and Ctf1β bind to an oppositely oriented palindrome, 5'-GCC(n2)GGC, in *F. solani* (Kämper et al. 1994), and FvCtf1α can bind a canonical palindrome 5'-GGC(n3)GCC with *FvCUT4* in *F. verticillioides*. The GC-rich palindrome is essential for cutinase induction by cutin monomers. Induction and enhancement of *FvCUT1* occur by binding the GC-rich (GCGCCSC) region at its promoters, resembling a positive-acting G-rich Sp1-like element in an enhancer in numerous viral and mammalian promoters (Jones et al. 1986). They also appear in the promoters of the *A. nidulans PGKA* and *GPDA* genes, which encode phosphoglycerate kinase and glyceraldehyde-3-phosphate dehydrogenase, respectively (Hoskins et al.1994). There are two binding sites in some cutinase genes: a silencing sequence that keeps basal gene expression low and affects cutinase gene inducibility and a G-rich positive-acting Sp1-like element that restores high expression levels by antagonizing the silencer. However, the G-rich activator from *F. solani* did not function as a true enhancer (Kämper et al. 1994). *FvCUT1* was highly induced under low H_2O_2 stress, suggesting that the GC-rich element plays a role in inducing enhancers for cutin induction with low H_2O_2 stress. *FvCUT1* is consistent with the high expression of chitin monomers through FvCtf1α binding to the GC-rich element. Isolation and characterization of other Ctf1α and PBP proteins, as well as the silencer- and activator-binding proteins, are necessary to further elucidate the mechanisms of cutinase gene regulation in *F. verticillioides*. On the other hand, FvCtf1α can bind to the CAMCA DNA element regions of 5 *FvFUM* genes promoters, *FvFUM1, 2, 6, 14, 16* genes, as detected by Multiple EM for Motif Elicitation (MEME) software. The conditions for CAMCA binding also need further exploration. Therefore, we speculated that FvCtf1α is a non-specific transcription factor with multiple promoter binding sites. In addition to bind to the inducible cutin gene promoter site GCGCCSC, it has

also been found for the first time to bind to the promoter site CAMCA of *FUM* related genes. FvCtf1α regulates the transcription of inducible cutinase to regulate pathogenicity and also regulates the transcription of key *FUM* genes to regulate FB1 production. Overall, our results provide new insights into the mechanism of FvCtf1α-mediated gene regulation in *F. verticillioides* pathogenesis and FB1 production. This study will provide a theoretical basis for reducing the toxicity and yield loss due to *F. verticillioides*.

Interpretations of data on fungal cutinase activity and pathogenicity are contradictory, and range from cutinase having no apparent influence on pathogenicity to enhancing the adhesion of fungal spores to the plant surface (Schäfer 1993). Different cutinase transcription factors *CTF* and *CUT* genes were expressed under various conditions. Ctf1β is involved in the constitutive expression of *CUT2* in the virulent strain *F. solani*, and its competitor CPBP cannot bind to palindrome 1 of *CUT2*, thus *CUT2* is not repressed (Li et al. 2002). However, in the saprophytic fungus *A. nidulans*, either glucose or starch can strongly repress the expression of *AnCUT2* (Castro-Ochoa et al. 2012). Later, the researchers discovered that lipid metabolism transcription factors (TFs) FarA regulated *AnCUT2* and FarB regulated *AnCUT3* (Bermúdez-García et al. 2019). However, *CUT2* was not detected virulence in the *F. verticillioides* strain under the tested conditions. We suggested that *FvCUT2* was repressed in CM medium with glucose and in maize kernel with starch. FvCtf1α indirectly regulates constitutive cutinase *FvCUT3*, and FvCtf1α interacts with FvFarB, suggesting that FvCtf1α may indirectly regulate *FvCUT3* through FvFarB. FarA also regulated *AnCUT1*, while NapA regulated *AnCUT4* in *A. nidulans* (Bermúdez-García et al. 2019).

F. solani f. sp. *pisi CUT1* is also under glucose catabolite repression, and its expression is highly induced by cutin monomers and is positively regulated by Ctf1α (Li et al. 2002). *F. solani* palindrome-binding protein (PBP) contains a zinc finger motif that shares homology with those in mammals, *Saccharomyces cerevisia*e, *Neurospora crassa*, and *Ustilago maydis* (Li and Kolattukudy 1995). *F. solani* PBP is believed to interfere with the binding of Ctf1α, the transcription factor involved in induction, to the *CUT1* promoter, and thus keeping the *CUT1* gene repressed until induced by cutin monomers (Lin et al. 2022). That is, Ctf1α competes with PBP for the binding site on the promoter of the inducible chitinase gene, and Ctf1α binding induces expression while PBP binding inhibits expression. For example, the expression of inducible *FvCUT1* was inhibited in CMII medium containing glucose, but was induced by cutin of maize based on RNA-seqencing data (Table 1). In our work, we found

that FvCtf1α directly regulates cutinase (*FvCUT1* and *FvCUT4*) induction. Cutin monomers, generated by low levels of constitutively expressed cutinase, induce high levels of cutinase that can help pathogenic fungi penetrate into the host through the cuticle, whose major structural polymer is cutin. We suggest that low levels of *F. verticillioides FvCUT3* induce Ctf1α regulated high levels of cutinase *FvCUT1* and *FvCUT4*, which collaborate with the degradation of the host cutin to cause disease.

It is also important to recognize that the regulatory mechanisms of CTFs are involved in many biochemical metabolic pathways. In *F. oxysporum*, the CTF regulates the expression of cutinase and other enzymes involved in fatty acid hydrolysis. In *A. oryzae*, a Zinc finger TF involved in lipid metabolism affects the expression levels of cutinase and other lipolytic enzymes (Garrido et al. 2012). The lipid metabolism transcription factors FarA for *AnCUT1* and *AnCUT2*, and FarB for *AnCUT3*, are involved in constitutive expression (Ramírez 2009). The phylogenetic tree showed that FvCtf1α was closer to FoCtf1α. Although both FoCtf1α and FvCtf1α regulate the transcription of cutin and lipase, FvCtf1α regulates pathogenicity while FoCtf1α does not. However, the homologous proteins of *F. solani* Ctf1α and Ctf1β are the same as FvCtf1α in the genome database of *F. verticillioides*. Ctf1α regulates β-oxidation and redox metabolism in *C. albicans* (Ramírez 2009), and the expression of a cutinase from *Monilinia fructicola* was enhanced using low H_2O_2 stress with cutin induction (Lee et al. 2010). Ctf1α responds to low H_2O_2 stress metabolic pathways and regulates the expression of these two genes (*FvCUT1* and *FvCUT4*). This is different from the transcription regulatory process in *A. nidulans*, which involves NapA functioning on *AnCUT4* under low H_2O_2 stress with cutin (Bermúdez-García et al. 2019). FvCtf1α regulates the expression of cell wall chitin synthase (Chs) in *F. verticillioides*. Three *MoCHSs* (*CHS1*, *CHS6*, and *CHS7*) in *M. oryzae* were found to be important for plant infection (Kong et al. 2012). It is need to further confirm whether the pathogenicity of *F. verticillioides* is related with FvCtf1α regulating FvChs.

Pathogens use enzymes such as lipases and cutinases to facilitate their penetration through the plant cuticle (Voigt et al. 2005; Hynes et al 2006; Srivastava et al. 2012). Prolonged pathogen adhesion promotes tighter and steadier attachment between the plant cuticle and spores, as they secrete a polysaccharide-based extracellular mucilaginous matrix, including pectinases, cellulases, and cutinases, towards the plant surface during the infection stage of spore germination on the host plant cuticle (Deising et al. 1992;Doss 1999). FvCtf1α may also affect its pathogenicity through a decrease in cell wall degradation enzyme capacity and spore production. The dormant

Peng *et al. Phytopathology Research*   (2024) 6:48

Page 14 of 18

spores of pathogenic fungi contain "constitutive-type" cutinases, previously also termed "sensing" cutinases, which release small amounts of cutin monomers from the host plant cuticle in a spatially localized manner (Köller et al. 1982). These cutin monomers are essential for subsequent stages of infection (Deising et al. 1992; Arya and Cohen 2022). "Constitutive-type" cutinase activity has been detected during the early stages of infection in the dormant spores of fungal species with different infection strategies, such as *Botrytis cinerea*, *Fusarium graminearum*, *Curvularia lunata*, *Pyrenopeziza brassicae*, *M. grisea*, and *Colletotrichum* spp. (Leroch et al. 2013; Liu et al. 2016; Davies et al. 2000; Oliver and Ipcho 2004; Auyong et al. 2015; Skamnioti and Gurr 2007). "Constitutive-type" cutinase FvCut3 has been detected in early infection strategies and affects pathogenicity. FvCtf1α and "constitutive-type" cutinase FvCut3 affect pathogenicity, but FvFarB does not. This suggests that the interaction between FvCtf1α and FvFarB may play a major role in affecting the expression of *FvCUT3* and subsequently impact pathogenicity. Further studies are needed to confirm this. In all, FvCtf1α, its induced cutinase FvCut4, and "constitutive-type" cutinase FvCut3 co- regulated cutin recognition in host leaves, the release of cutinase, causing leaf infection and subsequent water-logging.

Conclusion

In summary, our results demonstrate that the *F. verticillioides* transcription factor FvCtf1α regulates cutinase gene expression under cutin induction with low oxidative stress. It is also involved with fatty acid metabolism, carbon source utilization, cell wall integrity, conidiation, pathogenicity, fumonisin synthesis, and *FvFUM* genes expression. The Δ*Fvctf1α* mutant grown on inducing substrates failed to activate extracellular cutinolytic activity, nor to transcribe *FvCUT1*, *FvCUT4*, and *FvFUM1*, *FvFUM2*, *FvFUM6*, *FvFUM14*, *FvFUM16* genes. Our results suggest that FvCtf1α is a broad regulatory factor, acting not only on cellular degradation enzymes but also on genes related to FB1 toxin synthesis. Our results provide new insights into the mechanism of FvCtf1α-mediated gene regulation in *F. verticillioides* pathogenesis, which could be used as new effective strategies for controlling corn ear rot.

Methods
Bioinformatics and phylogenetic analyses

The full sequences of cutinase transcription factor genes (*FvCTF1α*, *FvFARA*, and *FvFARB*), cutinase genes, and other FvCtf1α target genes were downloaded from the National Center for Biotechnology Information (NCBI) by using homologous *F. solani* or *A. nidulans* protein sequence as queries. Protein domains were predicted using the SMART software (http://smart.emblheidelberg.de/). The nuclear signal was predicted using the NLS_Mapper software (http://nls-mapper.iab.keio.ac.jp/cgi-bin/NLS_Mapper_form.cgi). A phylogenetic tree was constructed using the MEGA 6.0 software, and the Maximum likelihood algorithm involving 1000 bootstrap replicates was employed.

Targeted gene deletion, complementation, and Southern blot assay

To further investigate the functions of *FvCTF1α* (FVEG_00228), the gene was replaced with hygromycin by homologous recombination (Lin et al. 2022). For complementation experiments, a fragment containing the *FvCTF1α* native promoter region and gene without the termination codon was ligated with the pKNTG vector and then transferred into the Δ*Fvctf1α* protoplast. The deletion (Δ*Fvctf1α*) and complementation (Δ*Fvctf1α-C*) strains were confirmed by PCR, qRT-PCR, and Southern hybridization. For Southern analysis, the genomic DNA isolated from the individual strains (*F. verticillioides* 7600, Δ*Fvctf1α*, and Δ*Fvctf1α*-C) was digested with *Eco*RI. The specific Southern hybridization probe was amplified from genomic DNA using primers of upstream flanking sequences (Additional file 1: Figure S2a), labeled, and subsequent hybridization and detection were performed according to a previously described protocol (Lin et al. 2022). Subsequently the validated strains were further chosen for functional characterization. Gene deletion and complementation of other target genes, *FvFARA*, *FvFARB*, *FvCUT3*, and *FvCUT*4, were performed using the same method described. All primers used in this study are listed (Additional file 2: Table S1).

Strains and culture conditions

F. verticillioides wild-type strain Fv7600 and all transformants were cultured on a minimal medium (MM) with 2% sucrose (Lin et al. 2022). To test the ability of Δ*Fvctf1α* strain to utilize various short carbon sources, it was inoculated in MM medium with 40 mM ethanol absolute, 40 mM sodium acetate, 20 mM glycerol, and 10 mM sodium butyrate as the sole carbon source, and the growth was observed after culturing at 28℃ for 3 days. In addition, to test the ability of Δ*Fvctf1α* to utilize long carbon sources, it was inoculated in MM medium with sucrose-containing long-chain fatty acids, including 3 mM linoleic acid, 3 mM sodium oleate, and 0.2% olive oil, respectively. The colony diameter was measured after 3 days of incubation. Cell wall integrity was tested by growing the Δ*Fvctf1α* strain on MM with sucrose supplemented with 100 mg/mL calcofluor white (CFW), 100 μg/mL Congo red (CR), or 0.01% sodium dodecyl sulfate (SDS).

Peng *et al. Phytopathology Research*   (2024) 6:48

Page 15 of 18

The tolerance of the Δ*Fvctf1α* strain to exogenous reactive oxygen species (ROS) was evaluated by measuring growth on MM with sucrose containing 10 mM H_2O_2. After 3 days of stress (CFW, CR, SDS, and H_2O_2) at 28℃, the colony diameter and inhibition were measured. After 3 days in PDA, the conidia of the strains were measured. Moreover, to further assay the relation between cutinase and low H_2O_2 stress, 0.1 mM H_2O_2 was added to 1% cutin medium (Lee et al. 2010). After 3 days of culture, the expression of cutinase, β-oxidation, and peroxisome biogenesis related genes were detected by qRT-PCR.

The expression of cutinase and other target genes detection and cell wall degrading enzyme assay. Crude cutin (1%) was added to MM liquid medium, and then wild-type *F. verticillioides* and the Δ*Fvctf1α* mutants were inoculated, and cultured at 28℃ with agitation (180 rpm). The expression levels of target cutinase genes at different cutin induction periods (cultured for 1, 2, 3, 4, 5, and 12 h) were detected by qRT-PCR. In addition, after 3 days of cultivation in an MM liquid medium, the expression levels of carbon metabolic-related genes and cell wall synthase genes in the strains were detected by qRT-PCR as previously described (Yu et al. 2022).

Wild-type *F. verticillioides* Fv7600, mutant strains Δ*Fvctf1α-25* and Δ*Fvctf1α-103*, and complement strain Δ*Fvctf1α-C* were inoculated in MM liquid medium containing 1% cutin, 1% pectin, and 1% carboxymethyl cellulose (CMC), respectively. The activities of cutinase, pectinase, and cellulase secreted by strains were detected after culturing at 28℃ and 150 rpm for 10 days. The supernatant of the culture was obtained after 5 min centrifugation at 4℃ and used as a crude enzyme preparation in the assay of CWDE cutinase activity, pectinase activity, and cellulase activity assay.

Extracellular cutinase activities were determined by the formation of yellow color p-nitrophenol butyrate (pNPB) after reaction with 5 mM paranitrophenyl butyrate dissolved in 50 mM potassium phosphate (pH 5.0) for 10 min and measured at A405 nm. Crude cutin was prepared from tomato fruit peel. Pectinase activity was determined using the 3,5-dinitrosalicylic acid (DNS) method, determining the amount of reducing sugar released from the substrates (Zhou et al. 2015). D-(+)-galacturonic acid monohydrate (Sigma) was used to generate a standard curve. Cellulase activity was determined by measuring the amounts of reducing sugar glucose released from 0.5% carboxymethyl-cellulose (CMC) with a 50 mmol/L pH 5.0 citrate buffer and reacted with DNS reagent under alkaline conditions (You and Chung 2007). The reducing sugar glucose was calculated using the standard curve.

GFP fusion and Bimolecular fluorescence complementation (BiFC) fluorescent experiment, confocal microscopy

To investigate the localization of FvCtf1α, FvFarA, and FvFarB, the recombinant fluorescent vectors (FvCtf1α-GFP, FvFarA-GFP, FvFarB-GFP) were constructed following our previously described method (Lin et al. 2022). *FvCTF1α*, *FvFARA*, and *FvFARB* genes with their native promoters were amplified from the genomic DNA of Fv7600, and the PCR products were cloned into the pKNT-GFP vector by one-step cloning, respectively. Each recombinant fluorescent vector was then transferred to its corresponding mutant. The positive transformants obtained from the corresponding mutants were stained with nuclear dye DAPI and observed with a confocal microscope (Nikon, Japan).

To investigate the interaction of FvCtf1α with FvFarA or FvFarB, the fluorescent vectors (FvCtf1α-NYFP, FvFarA-CYFP, FvFarB-CYFP) were constructed. *FvCTF1α* genes with their native promoter were cloned into the pKNT-NYFP vector with G418 resistance through a one-step cloning process. *FvFARA* and *FvFARB* genes with their native promoters were separately cloned into a pCX62-CYFP vector with hygromycin resistance via one-step cloning. Pairs of recombinant plasmids, FvCtf1α-NYFP with FvFarA-CYFP and FvCtf1α-NYFP with FvFarB-CYFP, were co-transformed into the wild-type Fv7600, respectively. BiFC fluorescence images were captured using a confocal laser scanning microscope (Nikon, Japan).

Pathogenicity assay and quantification of FB1 mycotoxin

The susceptible maize B73 and sugarcane Badila were used in pathogenicity assays. Toothpicks were soaked in the *F. verticillioides* spore suspension (1×10^6 conidia/mL). A needle was used to poke a hole in the middle section of the sugarcane internode, then inserted a toothpick soaked in the spore suspension, and finally wrapped the hole with a sealing film. After 7 dpi, the average area of sugarcane stem rot was calculated for statistical analysis. Moreover, 1 piece of mycelium block was inoculated onto the stem of a 2-week-old maize seedling, incubated at 28℃ in a greenhouse for 5 days, and the pathogenicity was observed. In addition, a mycelium block was inoculated onto the leaves of 4-week-old maize seedlings and incubated at 28℃ for 4 days to observe its pathogenicity. Tissue at the inoculation site was collected, and then the expression of disease-resistance genes was measured by qRT-PCR. This experiment was conducted with three independent biological replicates and analyzed statistically.

For the FB1 assay, spore suspension (1×10^6 conidia/mL) was inoculated on surface-sterilized B73 corn kernels for 10 days, and the FB1 content was quantified

using an FB1 ELISA Kit following the manufacturer's suggested protocol (Finder Biotech, Shenzhen). DNA from infected maize kernels was extracted to detect the infection amount of *F. verticillioides. F. verticillioides* biomass quantification was calculated by qRT-PCR based on the β-tubulin2 gene *TUB2* (FVEG_04081) standard curve. Meanwhile, the expression of FB1 biosynthesis genes in *F. verticillioides* by qRT-PCR were detected from infected maize kernels. Each experiment was repeated three times.

RNA sequencing and quantitative real-time PCR (qRT-PCR)

Maize kernels (B73) were processed in the same way as prepared for the FB1 assay. After 10 dpi, total RNA from infected kernels was extracted using the EastepTM Total RNA Extraction Kit (Promega, China) according to the manufacturer's instructions. The reagents were provided by the Illumina NextSeq 500 Kit, and sequencing was performed on an Illumina NextSeq 500 instrument (Illumina, USA). The sequenced reads were then filtered using PRINSEQ to ensure data quality. For subsequent identification of DEGs between the wild type and mutants, gene enrichment and functional annotation methods for DEGs, such as KOG (Clusters of Orthologous Groups of proteins in Eukaryotic), GO (Gene Ontology), and KEGG (Kyoto Encyclopedia of Genes and Genomes), were used as previously reported (Ye et al. 2018; Yu et al. 2022). Three biological replicates were conducted for each treatment.

Fungal total RNA was extracted using an RNA Kit 200 (OMEGA, USA), and cDNA templates were prepared with the TransScript® One-Step gDNA Removal and cDNA Synthesis SuperMix kit. The TransStart® Tip Green qPCR SuperMix (TransGen Biotech, China) was used to perform quantitative real-time PCR (qRT-PCR). The qRT-PCR detection of *F. verticillioides* and maize was standardized based on the expression levels of their respective housekeeping genes, *F. verticillioides TUB2* and maize B73 glyceraldehyde-3-phosphate dehydrogenase *GAPDH* (X07156). Data were obtained from three biological replicates.

Yeast one-hybrid assay and yeast two-hybrid assays

To detect the direct one-to-one regulatory relationship between transcription factor FvCtf1α and its regulatory genes, yeast one-hybrid experiments were conducted. The *FvCTF1α* cDNA sequence was ligated to pGADT7, and the pGADT7-FvCtf1α vector was constructed as prey. The Promoter 2.0 and BDGP websites (http://www.fruitfly.org/seq_tools/promoter.html) were used to predict the promoters of the tested target genes. The putative promoter of each detected target gene, including 100 bp upstream and downstream regions, was amplified and ligated to the pAbAi vector (Clontech) as bait. First, the pAbAi::pro vectors were transformed into Y1H-Gold (Clontech) cells, and the transformed strains were isolated on SD/-Ura medium and confirmed by PCR. Subsequently, the pGADT7-FvCtf1α vector was transformed into the previously constructed Y1H-Gold cells harboring the pAbAi::pro vector, and the transformants were isolated on SD/-Ura medium containing 0, 100, 150, 200 ng/mL Aureobasidin A (AbA). The transformants with pAbAi-p53 vector and pGADT7-p53 vector were used as positive controls.

To determine whether FvCtf1α exhibits self-activation function, yeast two-hybrid experiments were conducted following our previous protocol (Lin et al. 2022). The *FvCTF1α* cDNA sequence was cloned into pGBKT7 as the bait vector, and the empty pGADT7 vector was used as the prey vector. A pair of plasmids, pGBKT7-P53 and pGADT7-T, was used as a positive control, while another pair of plasmids, pGBKT7-Lam and pGADT7-T, served as a negative control.

Statistical analyses

Data were subjected to analysis of variance (ANOVA), and means were separated by the Least Significant Difference (LSD) test ($p < 0.05$).

Supplementary Information

Additional file 1: Figure S1. Sequence structure of FvCtf1α, FvFarA, FvFarB, and FvCut, and phylogenetic tree analysis of CTF transcription factors. **a** Schematic of FvCtf1α, FvFarA, and FvFarB of *F. verticillioides* showed a GAL4-like Zn(II)2Cys6 (purple) and a fungal specific transcription factor (blue). Sequence structure of CTF transcription factors identified by SMART software and their schematic were drawn using IBS 1.0 software, respectively. **b** The phylogenetic tree of Ctf1 was constructed based on the amino acid sequence from eight selected fungi including *M. oryzae* (*Mo*), *N. crassa* (*Nc*), and *F. verticillioides* (*Fv*), *F. oxysporum* (*Fo*), *Fusarium graminearum* (*Fg*), *Botrytis cinerea* (*Bc*), *C.albicans* (*Ca*), as well the orthologs from the fungus *F. solani* (*Fs*). Using the Clustal W method of the Megalign program, the tree was constructed using MEGA 6.0 software by Maximum Likelihood with 1000 bootstrap reapplication. Bootstrap support values greater than 50% are indicated at the relevant nodes and Bayesian posterior probabilities are ≥ 95%. The decimal under the branch indicates the degree of genetic variation of the gene. Numbers around nodes indicated the bootstrap value. The bar marker showed the genetic distance. **c** Schematic of four FvCut showed a SP (dark blue) and a cutinase catalytic domain (pink) in *F. verticillioides*. Sequence structure of FvCut was identified by SMART software and schematic were drawn using IBS 1.0 software. SP: signal peptide. **Figure S2.** Gene deletion and mutant complementation of cutinases transcription factor. **a** Diagram showing that the target gene coding region was replaced by the *HPH* cassette. *HPH*: Hygromycin. The upstream fragment is a probe used for hybridization. **b** PCR verification of knockout mutants Δ*Fvctf1α*. The ORF of the target gene *FvCTF1α* from the candidate transformant was amplified by PCR with no band appeared, and the connection product (UA) of the upstream fragment of the target gene and the *HPH* fragment was obtained by PCR. **c–e** Confirmation of the mutants by Southern blot. The genomic DNA is digested by different enzymes that of WT (Fv7600) and Δ*Fvctf1α* digested by *Eco*RI, that of WT and Δ*FvfarA* digested by *Bam*HI, that of

Peng *et al. Phytopathology Research* (2024) 6:48

Page 17 of 18

WT and Δ*FvfarB* were digested by *Hin*dIII, and then separated by agarose gel, respectively. Anticipated band sizes were obtained. **f–h** Confirmation of mutants and mutant complementation by qRT-PCR. qRT-PCR was used to quantify transcript level of *FvCTF1a*, *FvFARA*, and *FvFARB* genes by comparison with the reference gene β-tubulin2 using the $2^{-\Delta\Delta Ct}$ method. Error bars represent the standard deviation. ND means that the value is not detected. qRT-PCR was conducted at least twice with three independent biological replicates. **Figure S3.** Gene deletion of cutinases genes. **a**, **b** PCR verification of knockout mutants Δ*Fvcut3* and Δ*Fvcut4*. The ORF of the target gene *FvCUT3* and *FvCUT4* from the candidate transformant was amplified by PCR with no band appeared, and the connection product (UA) of the upstream fragment of the target gene and the *HPH* fragment was obtain by PCR, respectively. **c** qRT-PCR was used to confirm mutants. qRT-PCR was used to quantify transcript level of *FvCUT3* and *FvCUT4* genes by comparison with the reference gene β-tubulin2 using the $2^{-\Delta\Delta Ct}$ method. Error bars represent the standard deviation. ND means that the value is not detected. qRT-PCR was conducted at least twice with three independent biological replicates. **Figure S4.** FvCut3 and FvCut4 were not contributed to hype growth and pathogenicity on sugarcane. **a** The vegetative growths of Δ*Fvcut3*, Δ*Fvcut4*, and WT were monitored on CMII, MM medium, respectively. **b** Sugarcane (Badila) stem were split longitudinally to visually inspect rot symptoms 7 days after inoculation with wide type and Δ*Fvcut3*. **c** Sugarcane stem were split longitudinally to visually inspect rot symptoms 7 days after inoculation with wide-type and Δ*Fvcut4*. **Figure S5.** FvFarA and FvFarB were not contributed to hype growth and pathogenicity on sugarcane. **a** The vegetative growths of Δ*FvfarA*, Δ*FvfarB*, and WT were monitored on CMII, MM medium, respectively. **b** The colony diameters of the cultures were measured and analyzed by *t*-test. **c** Sugarcane were split longitudinally to visually inspect rot symptoms 7 days after inoculation. Sugarcanes were inoculated with immersed Δ*FvfarA*, Δ*FvfarB*, and WT conidia toothtips at the internodal region, respectively, and incubated for 7 days. Control were inoculated with sterile toothtip. Three independent biological repetitions were performed. **Figure S6.** The RNA-Seq analysis of the Δ*Fvctf1a* mutant. **a** Valcanic maps for Differential gene expression (DEGs) identified by 1.2-fold |log2_fold change| in FKPM values. DEGs analysis was conducted using cuffdiff v2.1.1 with parameters: -FDR(False Discovery Rate)=0.05 -library-norm-method classic-fpkm -u/-multi-read-correct -b/-frag-bias-correct. A gene that was considered to be differentially expressed must have at least 1.2-fold expression changes between WT and *Fvctf1a* mutant. Red dots, significantly upregulated genes. Green dots, significantly downregulated genes. Blue dots, nondifferentially expressed genes. **b**, **c** The enrich genes of DEGs by GO analysis, the x-axis displays the number of genes and the right y-axis shows GO terms, with the down-regulated DEGs enriching to 17 GO terms and the up-regulated DEGs enriching to 19 GO terms. **d**, **e** KEEG analysis of DEGs enrich pathway, the x-axis displays the number of genes and the right y-axis shows KEEG terms, with the down-regulated DEGs enriching to 20 pathways and the up-regulated DEGs enriched to 5 pathways.

Additional file 2: Table S1. The primers used in this study.

Availability of data and materials
Not applicable.

Declarations

Ethics approval and consent to participate
Not applicable.

Consent for publication
The authors agree to publish.

Competing interests
The authors declare no competing interests.

Author details
[1]Fujian Universities Key Laboratory for Plant-Microbe Interaction, College of Life Science, Fujian Agriculture and Forestry University, Fuzhou 350002, China. [2]Key Laboratory of Biopesticide and Chemical Biology of Education Ministry, Fujian Agriculture and Forestry University, Fuzhou 350002, China. [3]Marine Biotechnology Center, Fuzhou Institute of Oceanography, Minjiang University, Fuzhou 350108, China. [4]Fujian Provincial Key Laboratory of Crop Pest Monitoring and Control, Fuzhou 350122, China. [5]Public Technology Service Center, Fujian Medical University, Fuzhou 350122, China. [6]Department of Plant Pathology and Microbiology, Texas A&M University, College Station, TX 77843-2132, USA.

References

Arya GC, Cohen H. The Multifaceted Roles of Fungal Cutinases during Infection. J Fungi (Basel). 2022;8(2):199. https://doi.org/10.3390/jof8020199.

Auyong AS, Ford R, Taylor PW. The role of cutinase and its impact on pathogenicity of *Colletotrichum truncatum*. J Plant Pathol Microbiol. 2015;06(03):1000259. https://doi.org/10.4172/2157-7471.1000259.

Bermúdez-García E, Peña-Montes C, Martins I, Pais J, Pereira CS, Sánchez S, et al. Regulation of the cutinases expressed by *Aspergillus nidulans* and evaluation of their role in cutin degradation. Appl Microbiol Biotechnol. 2019;103(9):3863–74. https://doi.org/10.1007/s00253-019-09712-3.

Bin Yusof MT, Kershaw MJ, Soanes DM, Talbot NJ. FAR1 and FAR2 regulate the expression of genes associated with lipid metabolism in the rice blast fungus *Magnaporthe oryzae*. PLoS One. 2014;9(6):e99760. https://doi.org/10.1371/journal.pone.0099760.

Bravo-Ruiz G, Ruiz-Roldán C, Roncero MI. Lipolytic system of the tomato pathogen *Fusarium oxysporum* f. sp. lycopersici. Mol Plant Microbe Interact. 2013;26(9):1054–67. https://doi.org/10.1094/MPMI-03-13-0082-R.

Castro-Ochoa D, Peña-Montes C, González-Canto A, Alva-Gasca A, Esquivel-Bautista R, Navarro-Ocaña A, et al. ANCUT2, an extracellular cutinase from *Aspergillus nidulans* induced by olive oil. Appl Biochem Biotechnol. 2012;166(5):1275–90. https://doi.org/10.1007/s12010-011-9513-7.

Chen X, Li P, Liu H, Chen X, Huang J, Luo C, et al. A novel transcription factor UvCGBP1 regulates development and virulence of rice false smut fungus *Ustilaginoidea virens*. Virulence. 2021;12(1):1563–79. https://doi.org/10.1080/21505594.2021.1936768.

Davies KAA, De LI, Foster SJJ, Li D, Johnstone K, Ashby AMM. Evidence for a role of cutinase in pathogenicity of *Pyrenopeziza brassicae* on *Brassica*s. Physiol Mol Plant Pathol. 2000;57:63–75. https://doi.org/10.1006/pmpp.2000.0282.

Deising H, Nicholson RL, Haug M, Howard RJ, Mendgen K. Adhesion pad formation and the involvement of cutinase and esterases in the attachment of *Uredospores* to the host cuticle. Plant Cell. 1992;4(9):1101–11. https://doi.org/10.1105/tpc.4.9.1101.

Dennis GJ, Sherman BT, Hosack DA, Yang J, Gao W, Lane HC, Lempicki RA. DAVID: Database for Annotation, Visualization, and Integrated Discovery. Genome Biol. 2003;4(5):P3. https://doi.org/10.1186/gb-2003-4-9-r60.

Dickman MB, Padila GK, Kolattukudy PE. Insertion of cutinase gene into a wound pathogen enables it to infect intact host. Nature. 1989;342:446–8 https://doi.org/10.1038/342446a0.

Doss RP. Composition and enzymatic activity of the extracellular matrix secreted by germlings of *Botrytis cinerea*. Appl Environ Microbiol. 1999;65(2):404–8. https://doi.org/10.1128/AEM.65.2.404-408.1999.

Garrido SM, Kitamoto N, Watanabe A, Shintani T, Gomi K. Functional analysis of FarA transcription factor in the regulation of the genes encoding lipolytic enzymes and hydrophobic surface binding protein for the degradation of biodegradable plastics in *Aspergillus oryzae*. J Biosci Bioeng. 2012;113(5):549–55. https://doi.org/10.1016/j.jbiosc.2011.12.014.

Hurtado CA, Rachubinski RA. MHY1 encodes a C2H2-type zinc finger protein that promotes dimorphic transition in the yeast *Yarrowia lipolytica*. J Bacteriol. 1999;181(10):3051–7. https://doi.org/10.1128/JB.181.10.3051-3057.1999.

Hynes MJ, Murray SL, Duncan A, Khew GS, Davis MA. Regulatory genes controlling fatty acid catabolism and peroxisomal functions in the filamentous fungus *Aspergillus nidulans*. Eukaryot Cell. 2006;5(5):794–805. https://doi.org/10.1128/EC.5.5.794-805.2006.

Jones KA, Kadonaga JT, Luciw PA, Tjian R. Activation of the AIDS retrovirus promoter by the cellular transcription factor, Sp1. Science. 1986;232(4751):755–9. https://doi.org/10.1126/science.3008338.

Kämper JT, Kämper U, Rogers LM, Kolattukudy PE. Identification of regulatory elements in the cutinase promoter from *Fusarium solani* f. sp. pisi (*Nectria haematococca*). J Biol Chem. 1994;269(12):9195–204. https://doi.org/10.1016/0092-8674(94)90389-1.

Kolattukudy PE. Polyesters in higher plants. Adv Biochem Eng Biotechnol. 2001;71:1–49. https://doi.org/10.1007/3-540-40021-4_1.

Köller W, Allan CR, Kolattukudy PE. Protection of Pisum sativum from *Fusarium solani* f. sp. *pisi* by inhibition of cutinase with organophosphorus pesticides. Phytopathology. 1982;72:1425–30. https://doi.org/10.1094/phyto-72-1425.

Kong LA, Yang J, Li GT, Qi LL, Zhang YJ, Wang CF, et al. Different chitin synthase genes are required for various developmental and plant infection processes in the rice blast fungus *Magnaporthe oryzae*. PLoS Pathog. 2012;8(2):e1002526. https://doi.org/10.1371/journal.ppat.1002526.

Lee MH, Chiu CM, Roubtsova T, Chou CM, Bostock RM. Overexpression of a redox-regulated cutinase gene, *MfCUT1*, increases virulence of the brown rot pathogen *Monilinia fructicola* on *Prunus* spp. Mol Plant Microbe Interact. 2010;23(2):176–86. https://doi.org/10.1094/MPMI-23-2-0176.

Leroch M, Kleber A, Silva E, Coenen T, Koppenhöfer D, Shmaryahu A, et al. Transcriptome profiling of *Botrytis cinerea* conidial germination reveals upregulation of infection-related genes during the prepenetration stage. Eukaryot Cell. 2013;12(4):614–26. https://doi.org/10.1128/EC.00295-12.

Li D, Kolattukudy PE. Cloning and expression of cDNA encoding a protein that binds a palindromic promoter element essential for induction of fungal cutinase by plant cutin. J Biol Chem. 1995;270(20):11753–6. https://doi.org/10.1074/jbc.270.20.11753.

Li D, Kolattukudy PE. Cloning of cutinase transcription factor 1, a transactivating protein containing Cys6Zn2 binuclear cluster DNA-binding motif. J Biol Chem. 1997;272(19):12462–7. https://doi.org/10.1074/jbc.272.19.12462.

Li D, Sirakova T, Rogers L, Ettinger WF, Kolattukudy PE. Regulation of constitutively expressed and induced cutinase genes by different zinc finger transcription factors in *Fusarium solani* f. sp. pisi (*Nectria haematococca*). J Biol Chem. 2002;277(10):7905–12. https://doi.org/10.1074/jbc.M108799200.

Lin TS, Kolattukudy PE. Induction of a biopolyester hydrolase (cutinase) by low levels of cutin monomers in *Fusarium solani* f.sp. pisi. J Bacteriol. 1978;133(2):942–51. https://doi.org/10.1128/jb.133.2.942-951.1978.

Lin M, Abubakar YS, Wei L, Wang J, Lu X, Lu G, et al. *Fusarium verticillioides* Pex7/20 mediates peroxisomal PTS2 pathway import, pathogenicity, and fumonisin B1 biosynthesis. Appl Microbiol Biotechnol. 2022;106(19–20):6595–609. https://doi.org/10.1007/s00253-022-12167-8.

Liu T, Hou J, Wang Y, Jin Y, Borth W, Zhao F, et al. Genome-wide identification, classification and expression analysis in fungal-plant interactions of cutinase gene family and functional analysis of a putative *ClCUT7* in *Curvularia lunata*. Mol Genet Genomics. 2016;291(3):1105–15. https://doi.org/10.1007/s00438-016-1168-1.

Martinez C, De Geus P, Lauwereys M, Matthyssens G, Cambillau C. *Fusarium solani* cutinase is a lipolytic enzyme with a catalytic serine accessible to solvent. Nature. 1992;356(6370):615–8. https://doi.org/10.1038/356615a0.

Oliver RP, Ipcho SV. Arabidopsis pathology breathes new life into the necrotrophs-vs.-biotrophs classification of fungal pathogens. Mol Plant Pathol. 2004;5(4):347–52. https://doi.org/10.1111/j.1364-3703.2004.00228.x.

Peterbauer CK, Litscher D, Kubicek CP. The *Trichoderma* atroviride seb1 (stress response element binding) gene encodes an AGGGG-binding protein which is involved in the response to high osmolarity stress. Mol Genet Genomics. 2002;268(2):223–31. https://doi.org/10.1007/s00438-002-0732-z.

Poopanitpan N, Kobayashi S, Fukuda R, Horiuchi H, Ohta A. An ortholog of farA of *Aspergillus nidulans* is implicated in the transcriptional activation of genes involved in fatty acid utilization in the yeast *Yarrowia lipolytica*. Biochem Biophys Res Commun. 2010;402(4):731–5. https://doi.org/10.1016/j.bbrc.2010.10.096.

Ramírez MA, Lorenz MC. The transcription factor homolog CTF1 regulates beta-oxidation in *Candida albicans*. Eukaryot Cell. 2009;8(10):1604–14. https://doi.org/10.1128/EC.00206-09.

Rocha AL, Di Pietro A, Ruiz-Roldán C, Roncero MI. Ctf1, a transcriptional activator of cutinase and lipase genes in *Fusarium oxysporum* is dispensable for virulence. Mol Plant Pathol. 2008;9(3):293–304. https://doi.org/10.1111/j.1364-3703.2007.00463.x.

Schäfer W. The role of cutinase in fungal pathogenicity. Trends Microbiol. 1993;1(2):69–71. https://doi.org/10.1016/0966-842x(93)90037-r.

Skamnioti P, Gurr SJ. *Magnaporthe grisea* cutinase2 mediates appressorium differentiation and host penetration and is required for full virulence. Plant Cell. 2007;19(8):2674–89. https://doi.org/10.1105/tpc.107.051219.

Skamnioti P, Furlong RF, Gurr SJ. Evolutionary history of the ancient cutinase family in five filamentous ascomycetes reveals differential gene duplications and losses and in *Magnaporthe grisea* shows evidence of sub- and neo-functionalization. New Phytol. 2008;180(3):711–21. https://doi.org/10.1111/j.1469-8137.2008.02598.x.

Srivastava A, Ohm RA, Oxiles L, Brooks F, Lawrence CB, Grigoriev IV, et al. zinc-finger-family transcription factor, AbVf19, is required for the induction of a gene subset important for virulence in *Alternaria brassicicola*. Mol Plant Microbe Interact. 2012;25(4):443–52. https://doi.org/10.1094/MPMI-10-11-0275.

Sweigard JA, Chumley FG, Valent B. Disruption of a *Magnaporthe grisea* cutinase gene. Mol Gen Genet. 1992;232(2):183–90 PMID: 1557024.

Ueda H, Mitsuhara I, Tabata J, Kugimiya S, Watanabe T, Suzuki K, et al. Extracellular esterases of phylloplane yeast *Pseudozyma antarctica* induce defect on cuticle layer structure and water-holding ability of plant leaves. Appl Microbiol Biotechnol. 2015;99(15):6405–15. https://doi.org/10.1007/s00253-015-6523-3.

Ueda H, Kurose D, Kugimiya S, Mitsuhara I, Yoshida S, Tabata J, Suzuki K, Kitamoto H. Disease severity enhancement by an esterase from non-phytopathogenic yeast *Pseudozyma antarctica* and its potential as adjuvant for biocontrol agents. Sci Rep. 2018;8(1):16455. https://doi.org/10.1038/s41598-018-34705-z.

Ueda H, Tabata J, Seshime Y, Masaki K, Sameshima-Yamashita Y, Kitamoto H. Cutinase-like biodegradable plastic-degrading enzymes from phylloplane yeasts have cutinase activity. Biosci Biotechnol Biochem. 2021;85(8):1890–8. https://doi.org/10.1093/bbb/zbab113.

Van kan JA, van't Klooste JW, Wagemakers CA, Dees DC, van der Vlugt-Bergmans CJ. Cutinase A of *Botrytis cinerea* is expressed, but not essential, during penetration of gerbera and tomato. Mol Plant Microbe Interact. 1997;10(1):30–8. https://doi.org/10.1094/MPMI.1997.10.1.30.

Voigt CA, Schäfer W, Salomon S. A secreted lipase of *Fusarium graminearum* is a virulence factor required for infection of cereals. Plant J. 2005;42(3):364–75. https://doi.org/10.1111/j.1365-313X.2005.02377.x.

Woloshuk CP, Kolattukudy PE. Mechanism by which contact with plant cuticle triggers cutinase gene expression in the spores of Fusarium solani f. sp. pisi. Proc Natl Acad Sci U S A. 1986;83(6):1704–8. https://doi.org/10.1073/pnas.83.6.1704.

Ye J, Zhang Y, Cui H, Liu J, Wu Y, Cheng Y, et al. WEGO 2.0: a web tool for analyzing and plotting GO annotations, 2018 update. Nucleic Acids Res. 2018;46(W1):W71–5. https://doi.org/10.1093/nar/gky400.

You BJ, Chung KR. Phenotypic characterization of mutants of the citrus pathogen Colletotrichum acutatum defective in a PacC-mediated pH regulatory pathway. FEMS Microbial Lett. 2007;277(1):107–14. https://doi.org/10.1111/j.1574-6968.2007.00951.x.

Yu WY, Lin M, Yan HJ, Wang JJ, Zhang SM, Lu GD, et al. The peroxisomal matrix shuttling receptor Pex5 plays a role in FB1 production and virulence in *Fusarium verticillioides*. J Integr Agr. 2022;21(10):2957–72. https://doi.org/10.1016/j.jia.2022.07.044.

Zhang L, Guarente L. The yeast activator HAP1-a GAL4 family member-binds DNA in a directly repeated orientation. Genes Dev. 1994;8(17):2110–9. https://doi.org/10.1101/gad.8.17.2110.

Zhou C, Ye J, Xue Y, et al. Directed evolution and structural analysis of alkaline pectate lyase from the alkaliphilic bacterium *Bacillus* sp. strain N16-5 to improve its thermostability for efficient ramie degumming. Appl Environ Microbiol. 2015;81:5714–23. https://doi.org/10.1128/AEM.01017-15.